Multiple Exciton Generation in Si and Ge Nanoparticles with High Pressure Core Structures

S. Wippermann, M. Vörös, D. Rocca, A. Gali, G. Zimanyi, G. Galli

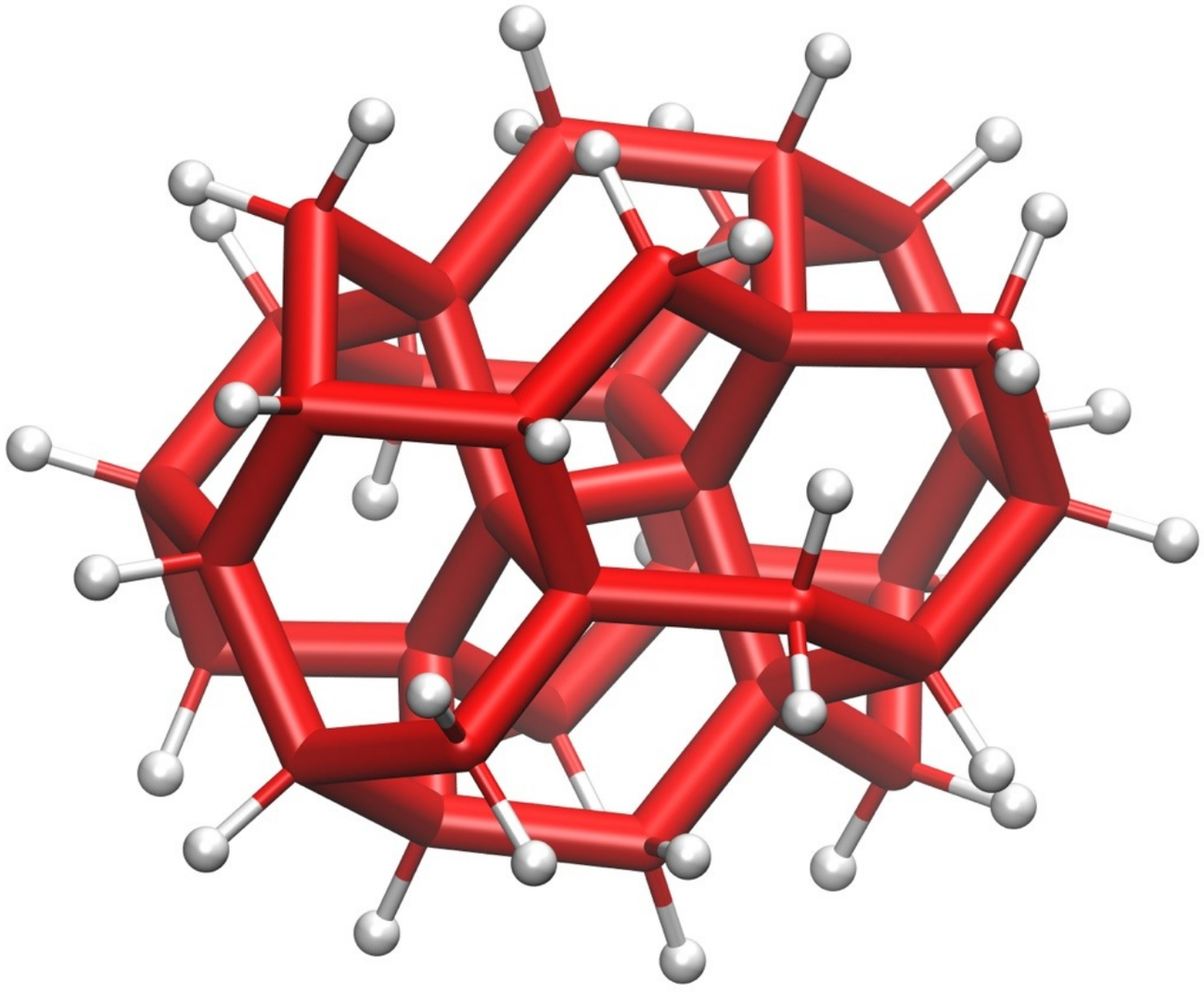

NanoMatFutur

Bundesministerium für Bildung und Forschung

MAX-PLANCK-GESELLSCHAFT

DPG-2014, 04/03/2014

Multiple Exciton Generation (MEG)

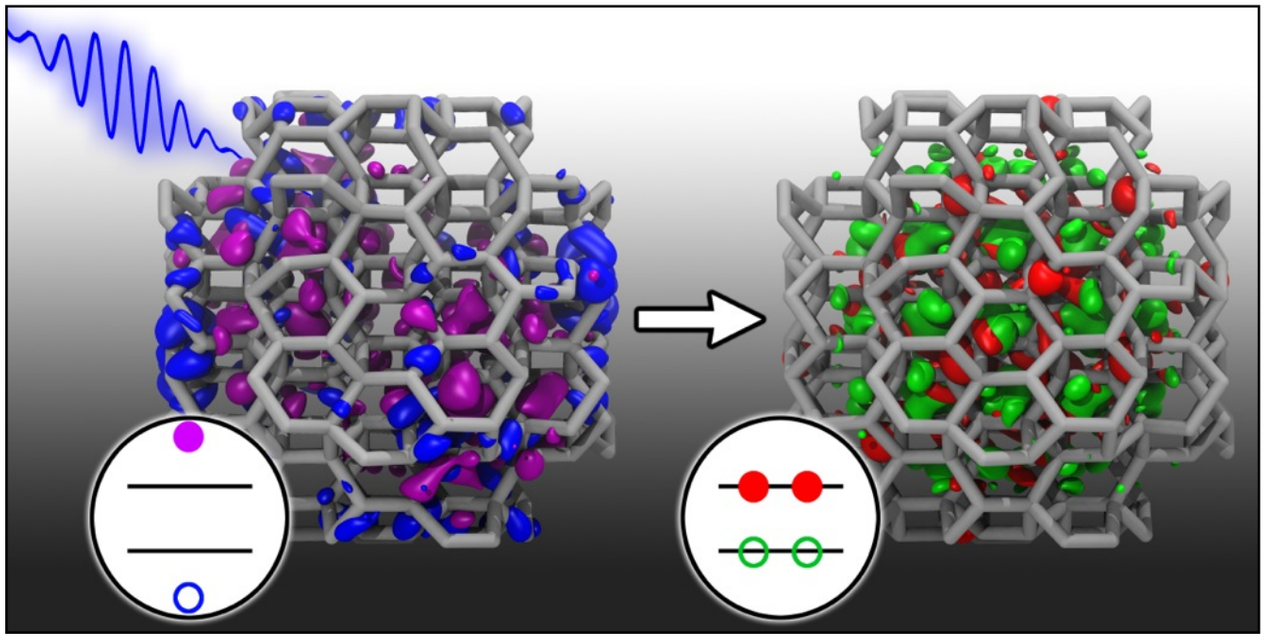

- **MEG:** hot exciton relaxes by exciting another exciton
- Promising pathway to exceed Shockley-Queisser limit in 3rd generation solar cells

[1] A. Nozik, Physica E **14**, 115 (2002)

Multiple Exciton Generation (MEG)

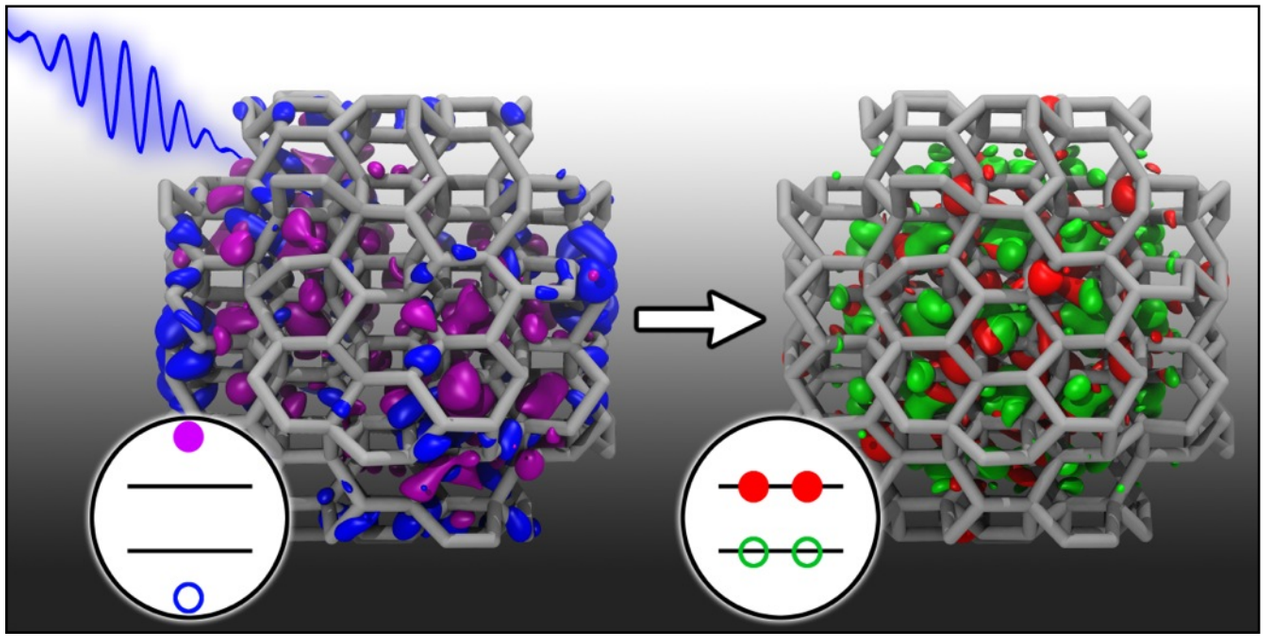

- **MEG:** hot exciton relaxes by exciting another exciton
- Promising pathway to exceed Shockley-Queisser limit in 3rd generation solar cells

M. Beard, JPCL **2**, 1282 (2011)

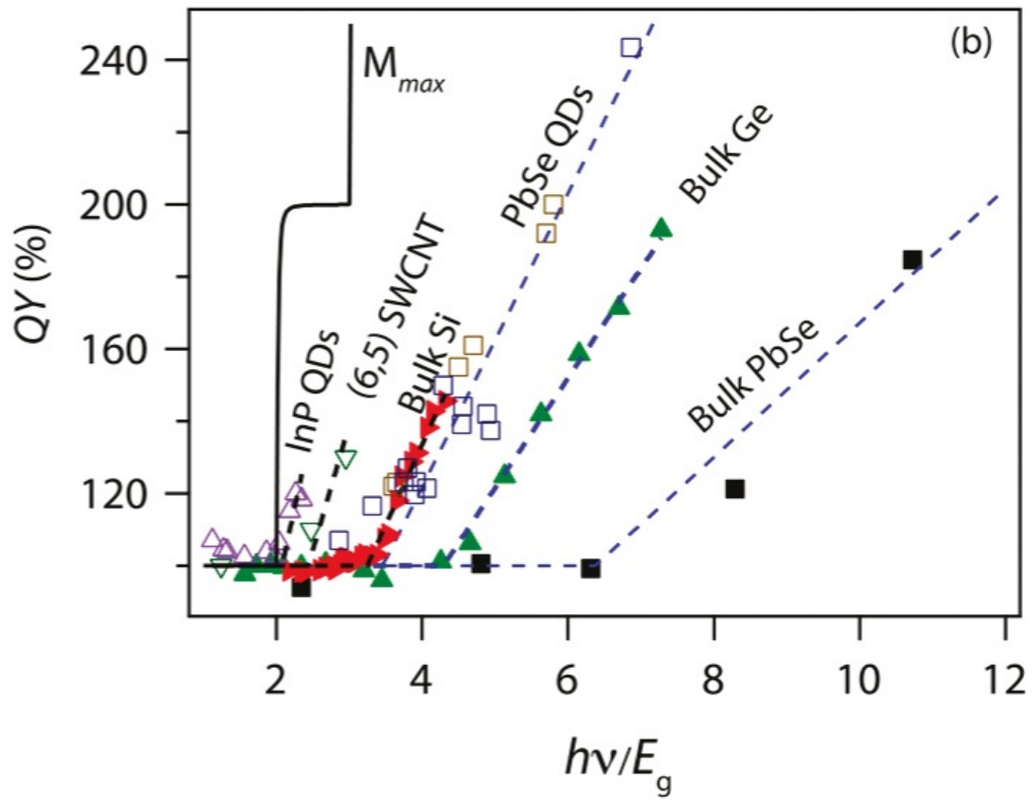

- enhanced MEG in quantum-confined nanostructures, e. g. nanocrystals

[1] A. Nozik, Physica E **14**, 115 (2002)

Multiple Exciton Generation (MEG)

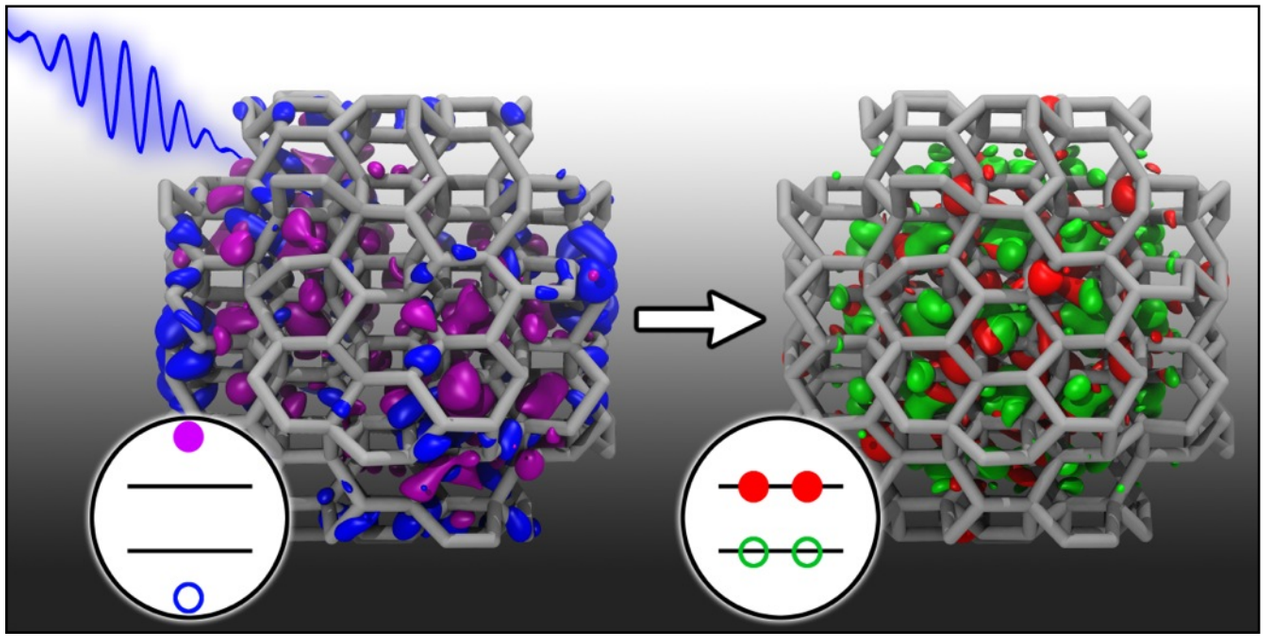

M. Beard, JPCL **2**, 1282 (2011)

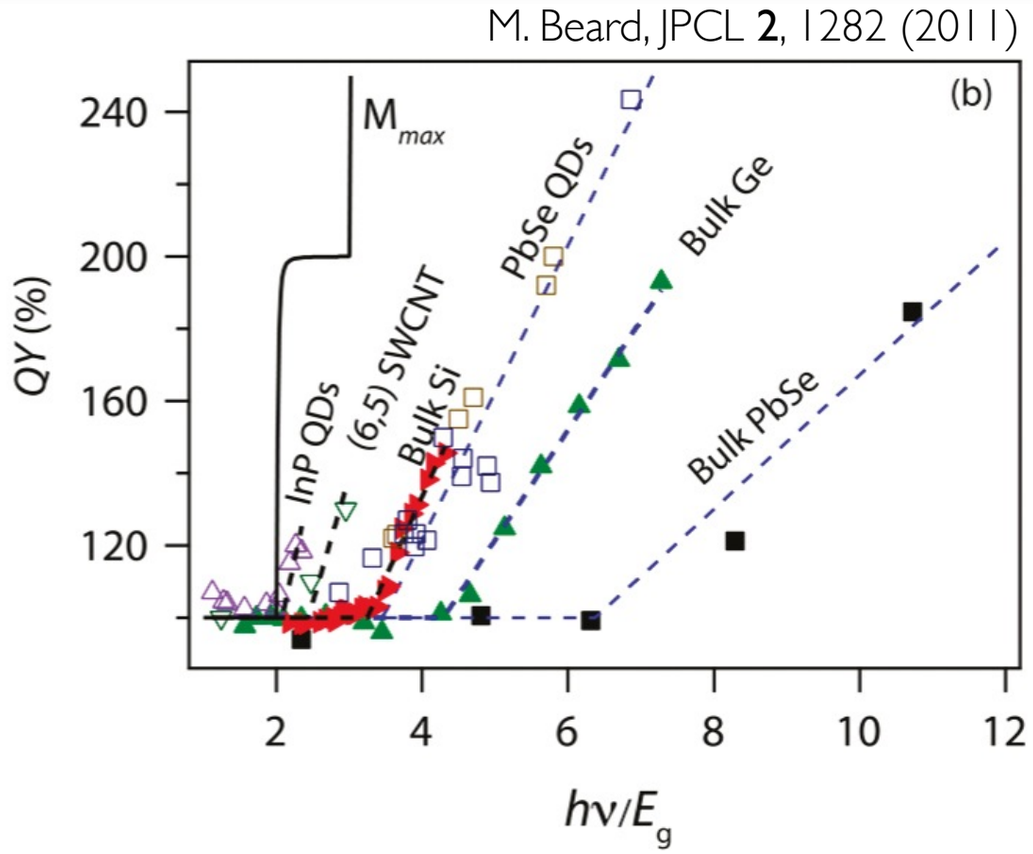

- **MEG:** hot exciton relaxes by exciting another exciton
- Promising pathway to exceed Shockley-Queisser limit in 3rd generation solar cells
- enhanced MEG in quantum-confined nanostructures, e. g. nanocrystals

Key problem

- Quantum confinement required for efficient MEG, but pushes electronic gap beyond solar spectrum
- MEG observed in Si and Ge: gap/wavefunction engineering possible?
  => investigate nanocrystals with high pressure core structures

[1] A. Nozik, Physica E **14**, 115 (2002)

Allotropes of Si and Ge

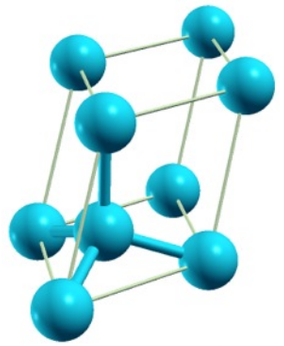

cubic diamond,
semiconductor

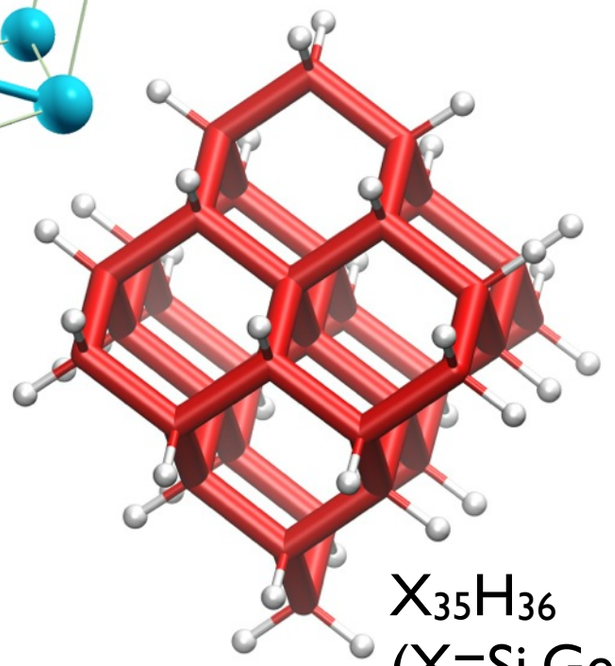

$X_{35}H_{36}$
(X=Si,Ge)

Allotropes of Si and Ge

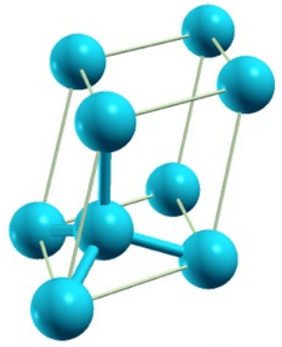

cubic diamond,
semiconductor

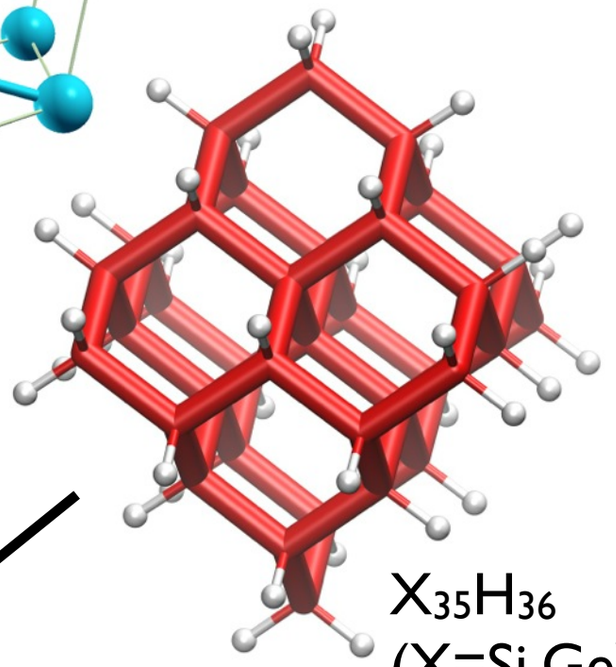

$X_{35}H_{36}$
(X=Si,Ge)

Si

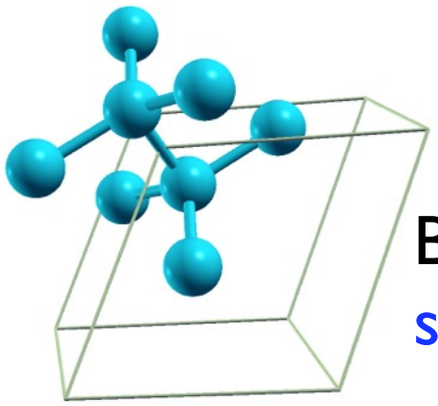

BC8,
semimetal

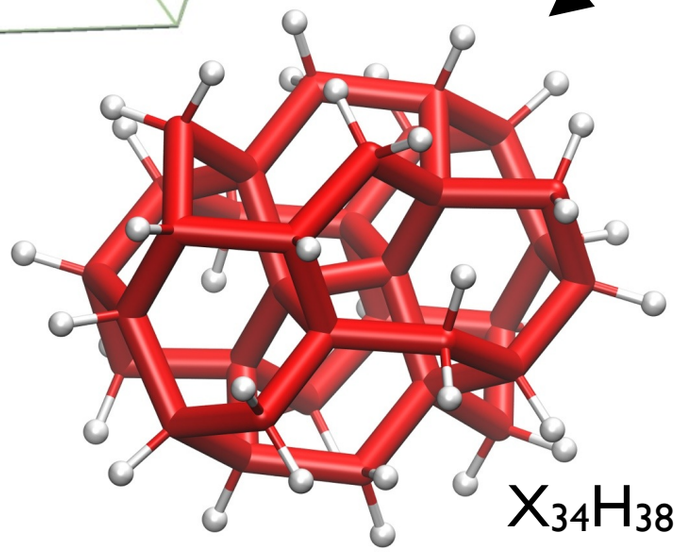

$X_{34}H_{38}$

[2] S. Ganguly *et al.*, J. Am. Chem. Soc. **136**, 1296 (2014)

Allotropes of Si and Ge

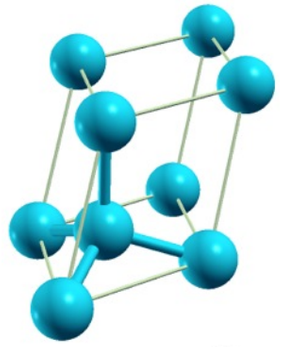

cubic diamond,
semiconductor

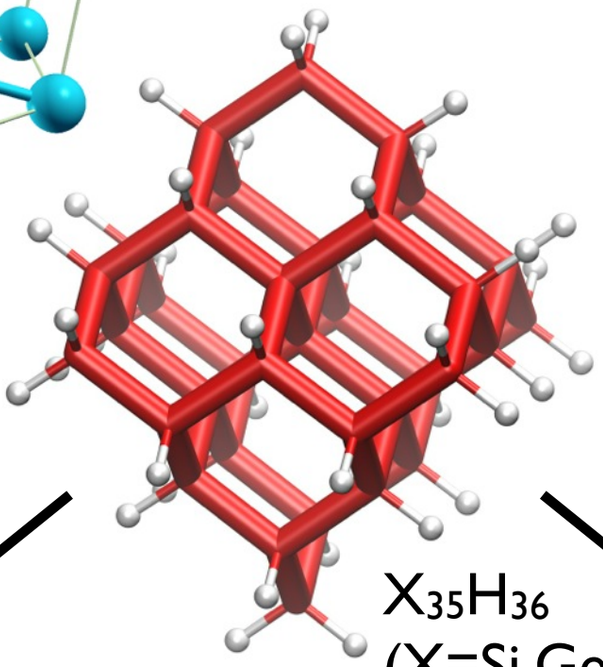

$X_{35}H_{36}$
(X=Si,Ge)

Si

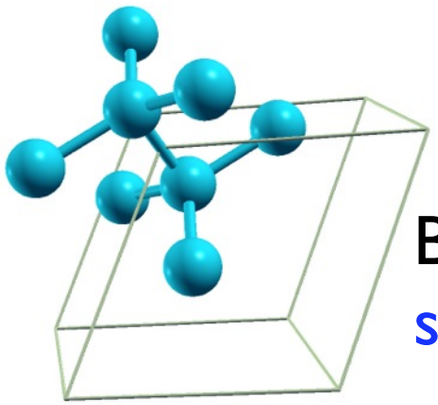

BC8,
semimetal

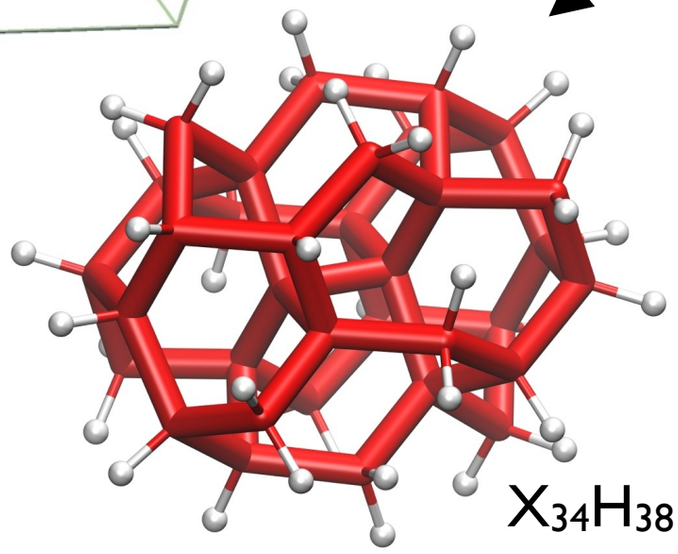

$X_{34}H_{38}$

Ge

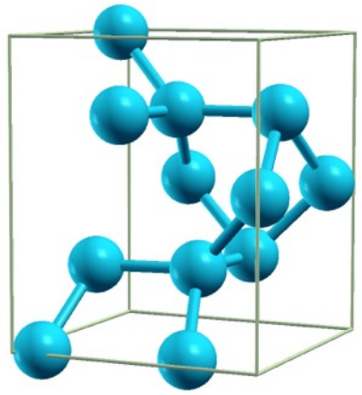

ST12

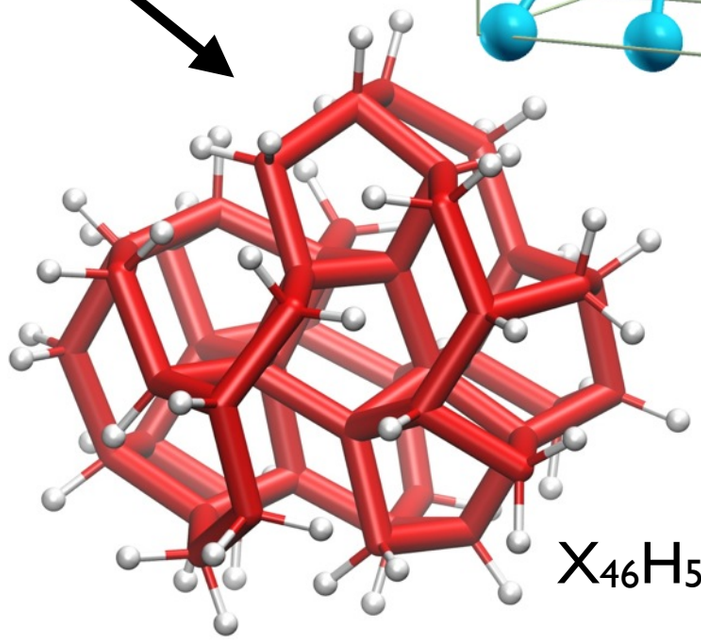

$X_{46}H_{52}$

[2] S. Ganguly *et al.*, J. Am. Chem. Soc. **136**, 1296 (2014)

[3] S. J. Kim *et al.*, J. Mater. Chem. **20**, 331 (2010)

Reduced gaps for BC8 and ST12 nanocrystals

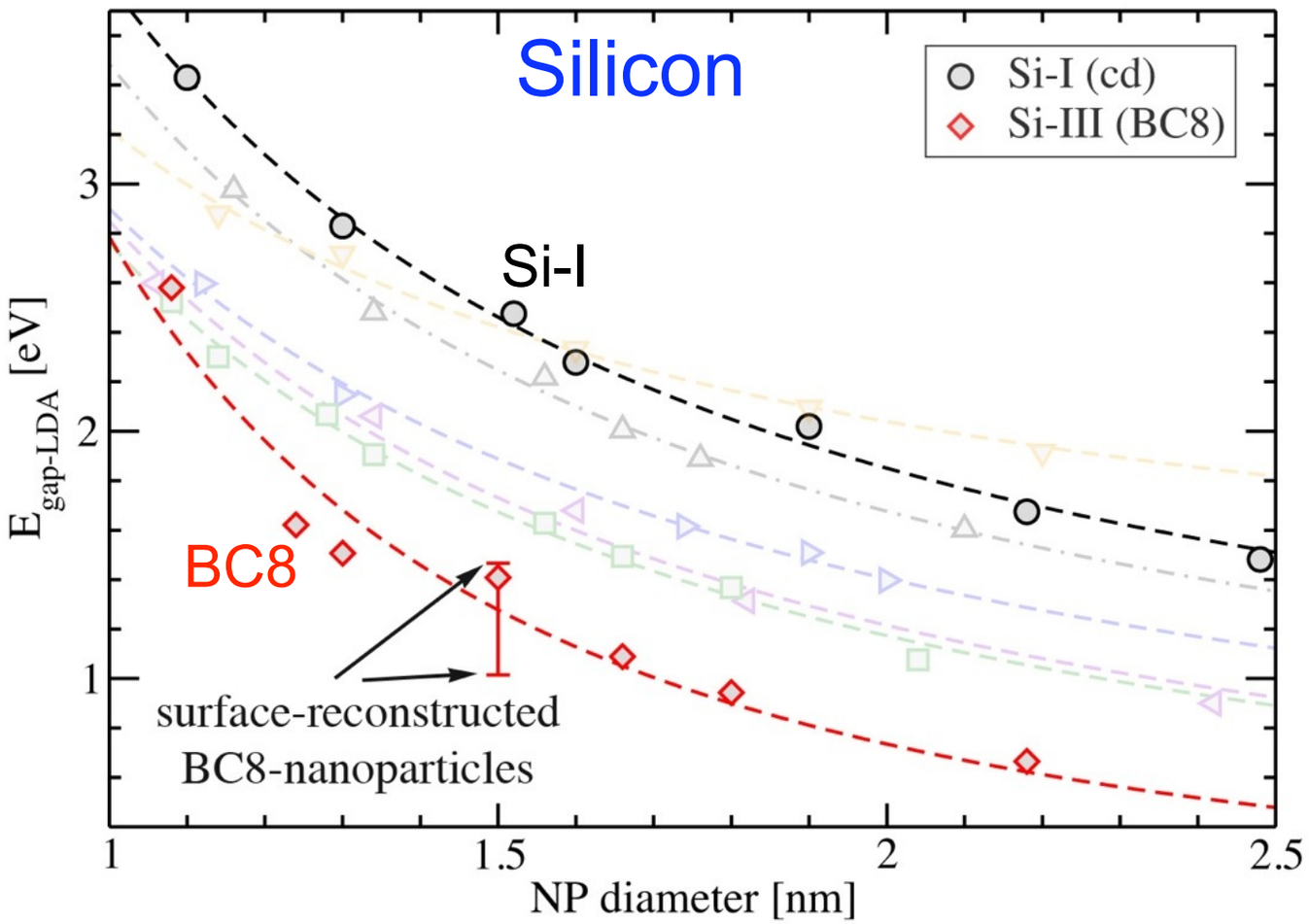

Reduced gaps for BC8 and ST12 nanocrystals

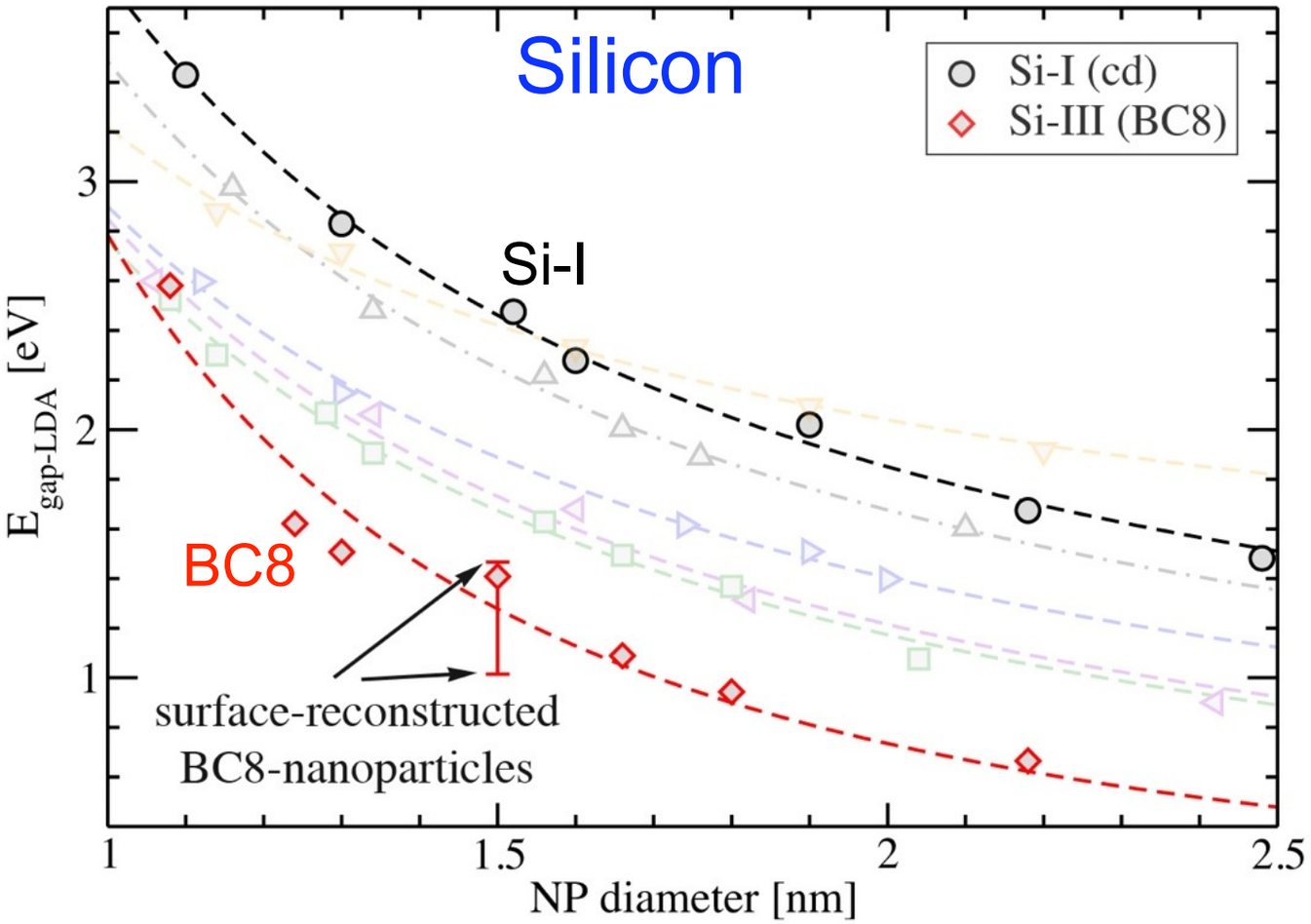

- BC8 is semimetal in the bulk, quantum confinement opens small gap in **BC8 nanocrystals => significantly reduced gaps compared to Si-I**

Reduced gaps for BC8 and ST12 nanocrystals

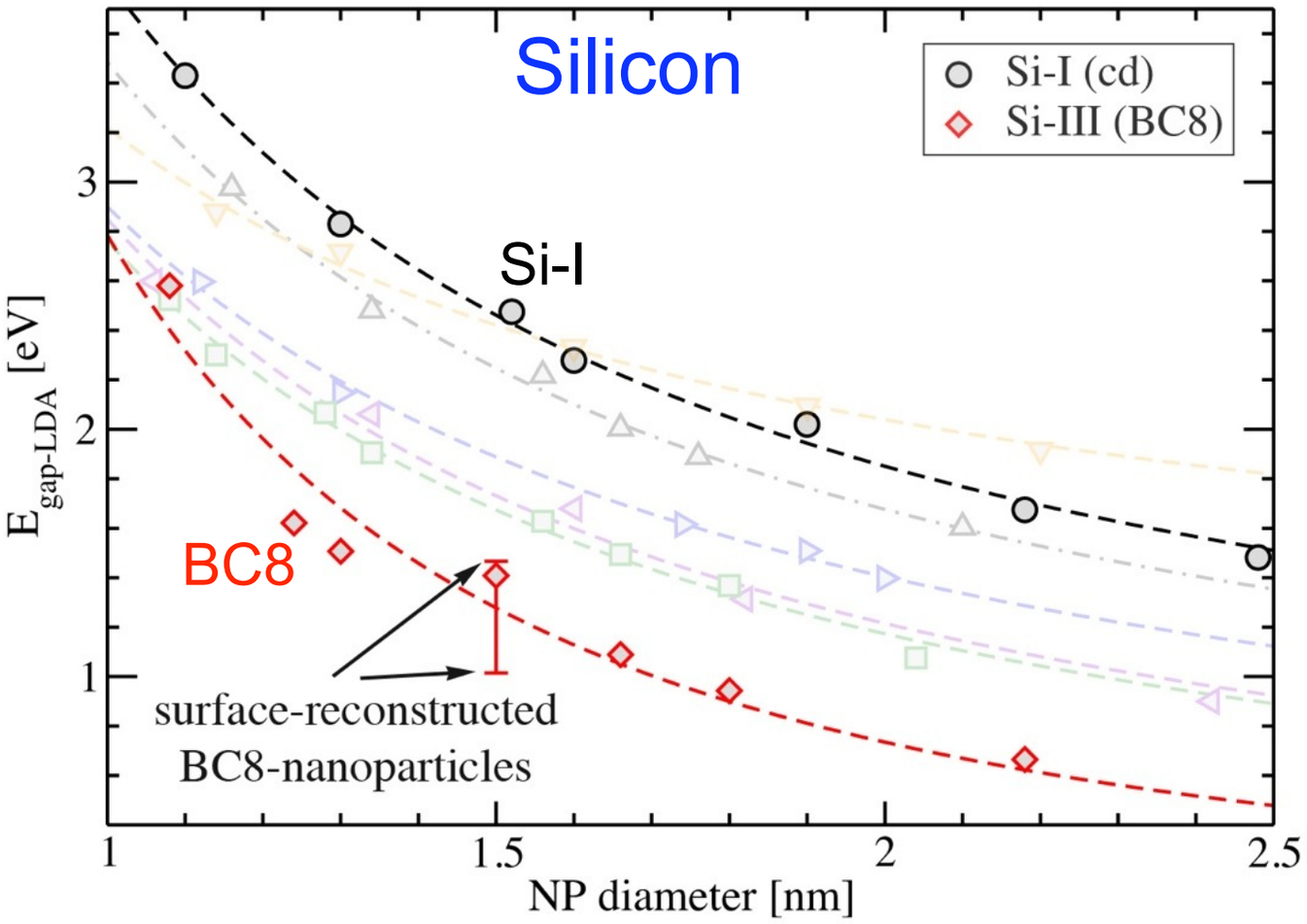

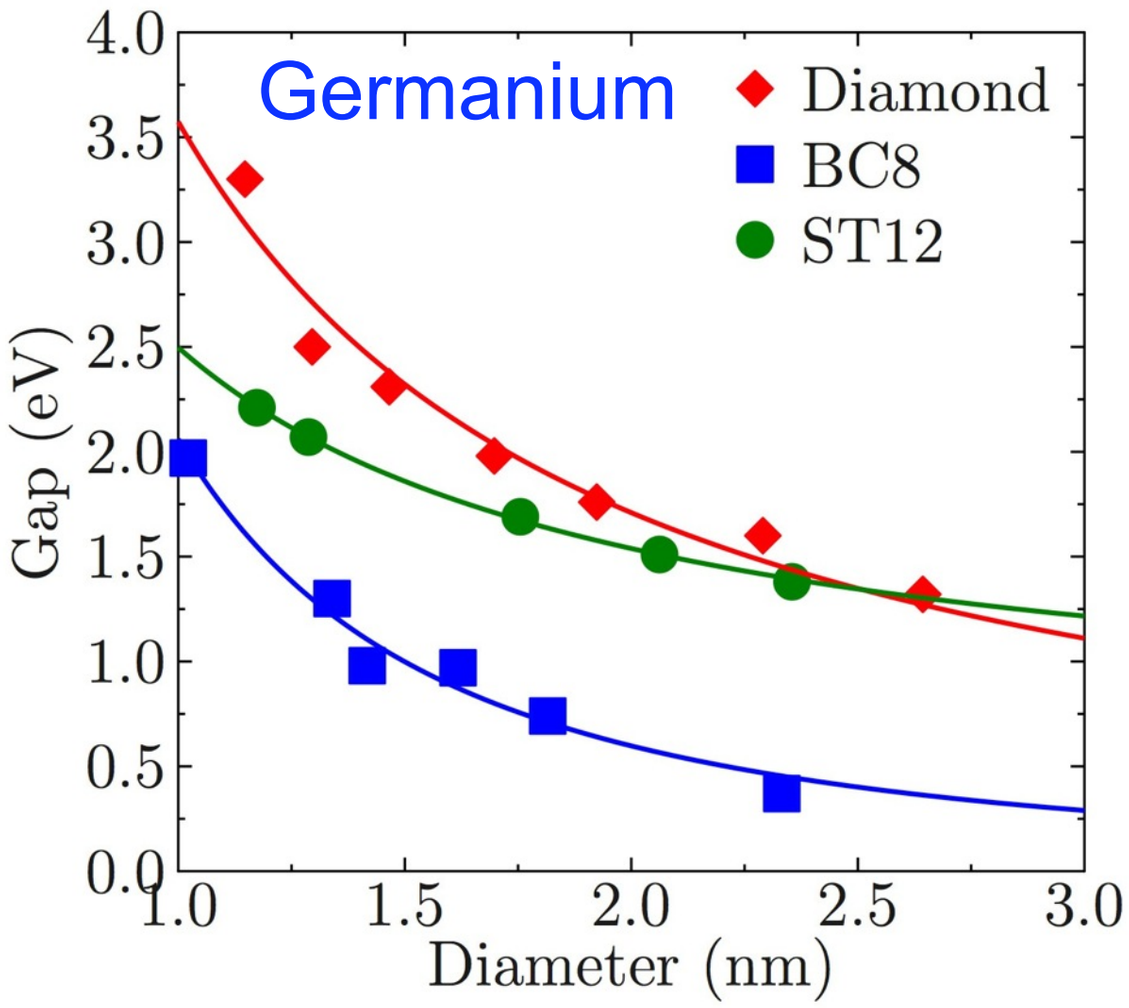

- BC8 is semimetal in the bulk, quantum confinement opens small gap in **BC8 nanocrystals => significantly reduced gaps compared to Si-I**

Reduced gaps for BC8 and ST12 nanocrystals

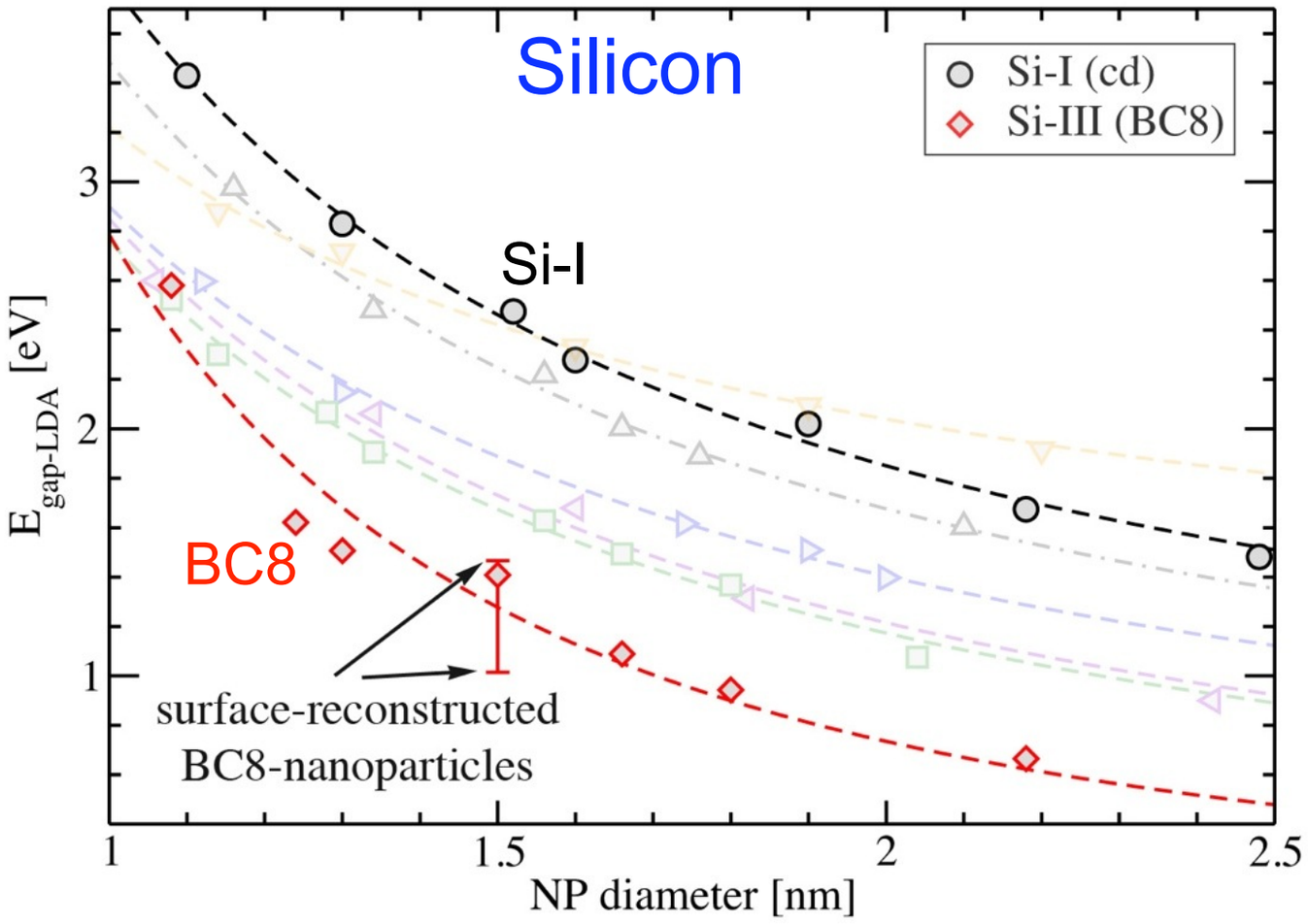

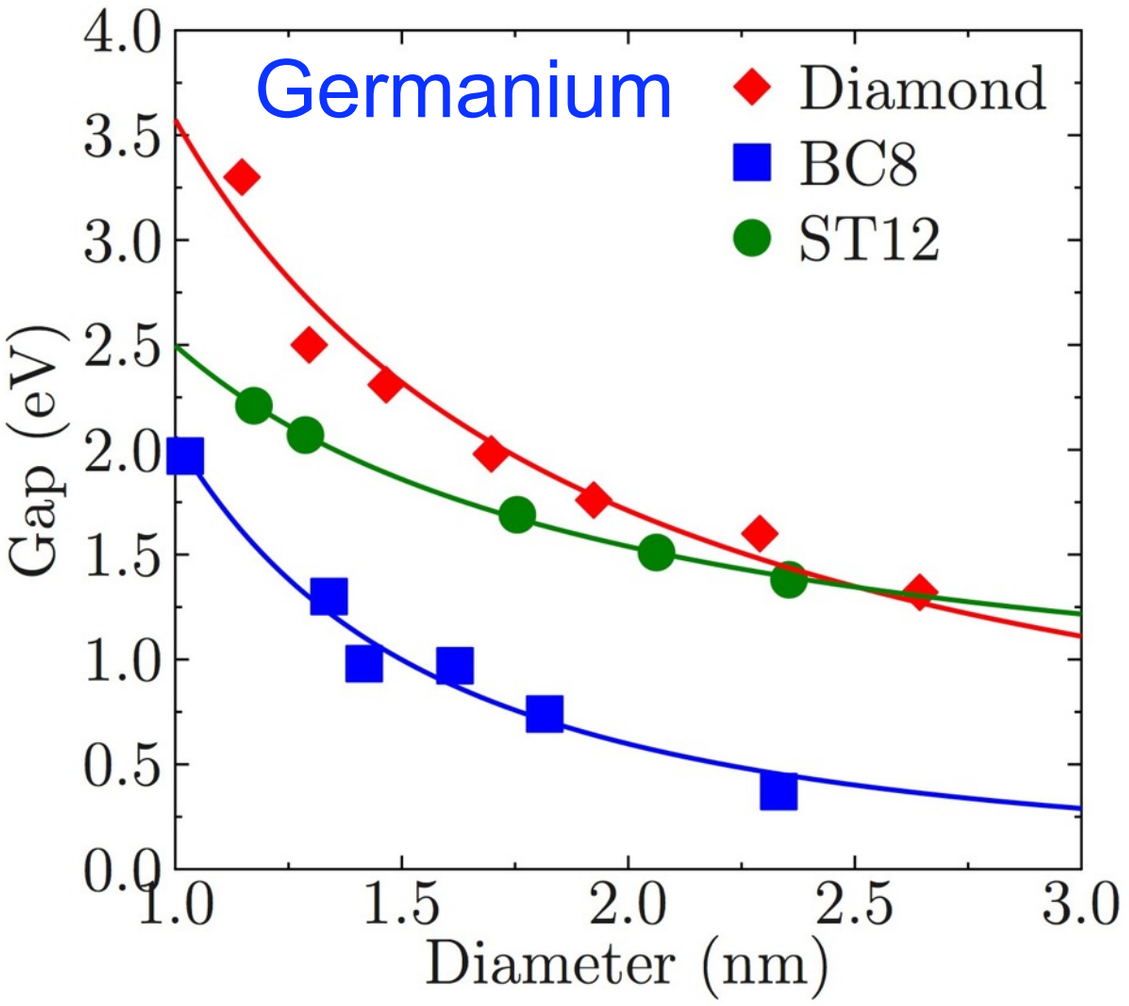

- BC8 is semimetal in the bulk, quantum confinement opens small gap in **BC8 nanocrystals => significantly reduced gaps compared to Si-I**
- Ge ST12 features reduced gaps for d < 2.5nm, significantly increased electronic density of states at band edges

Reduced gaps for BC8 and ST12 nanocrystals

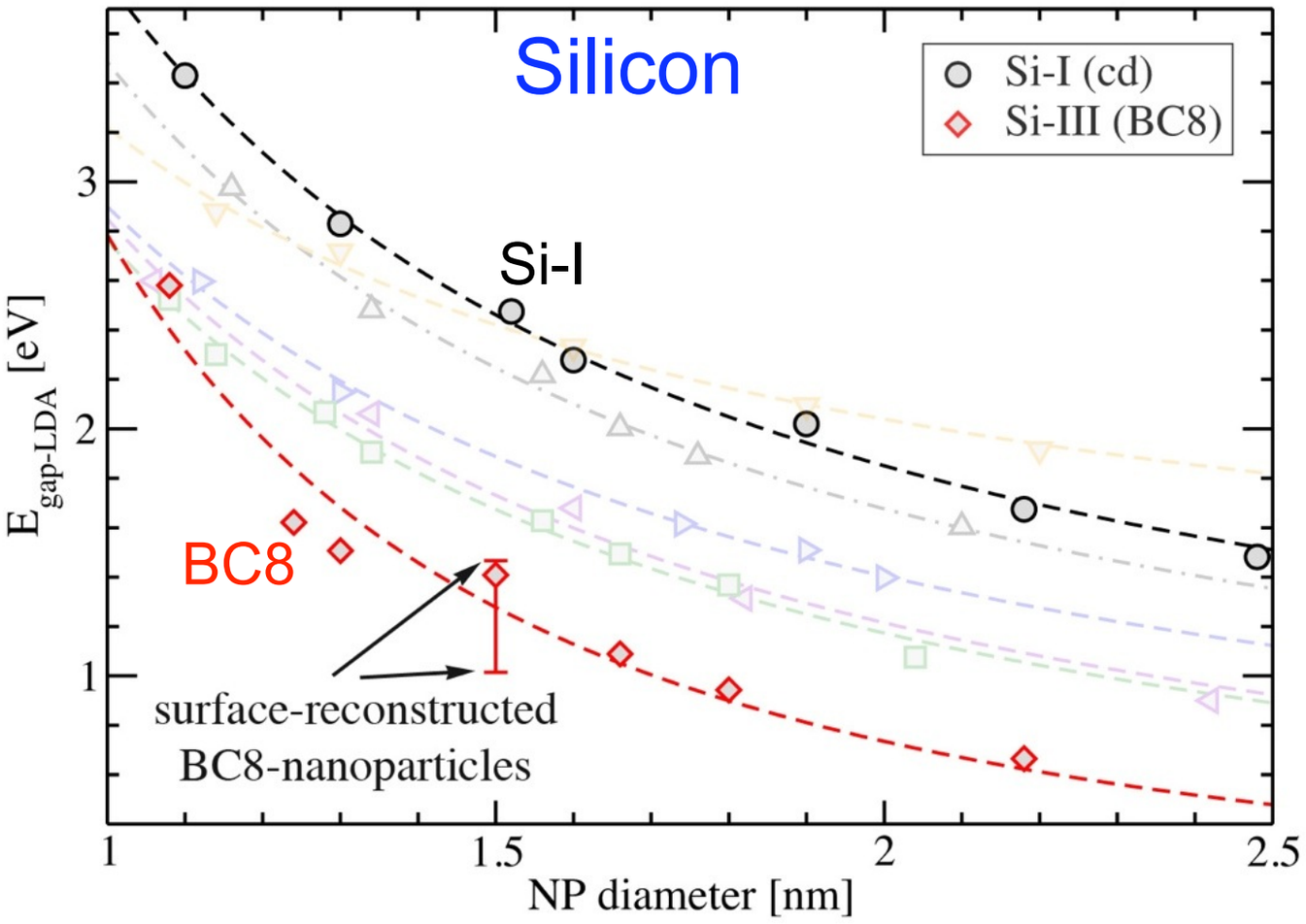

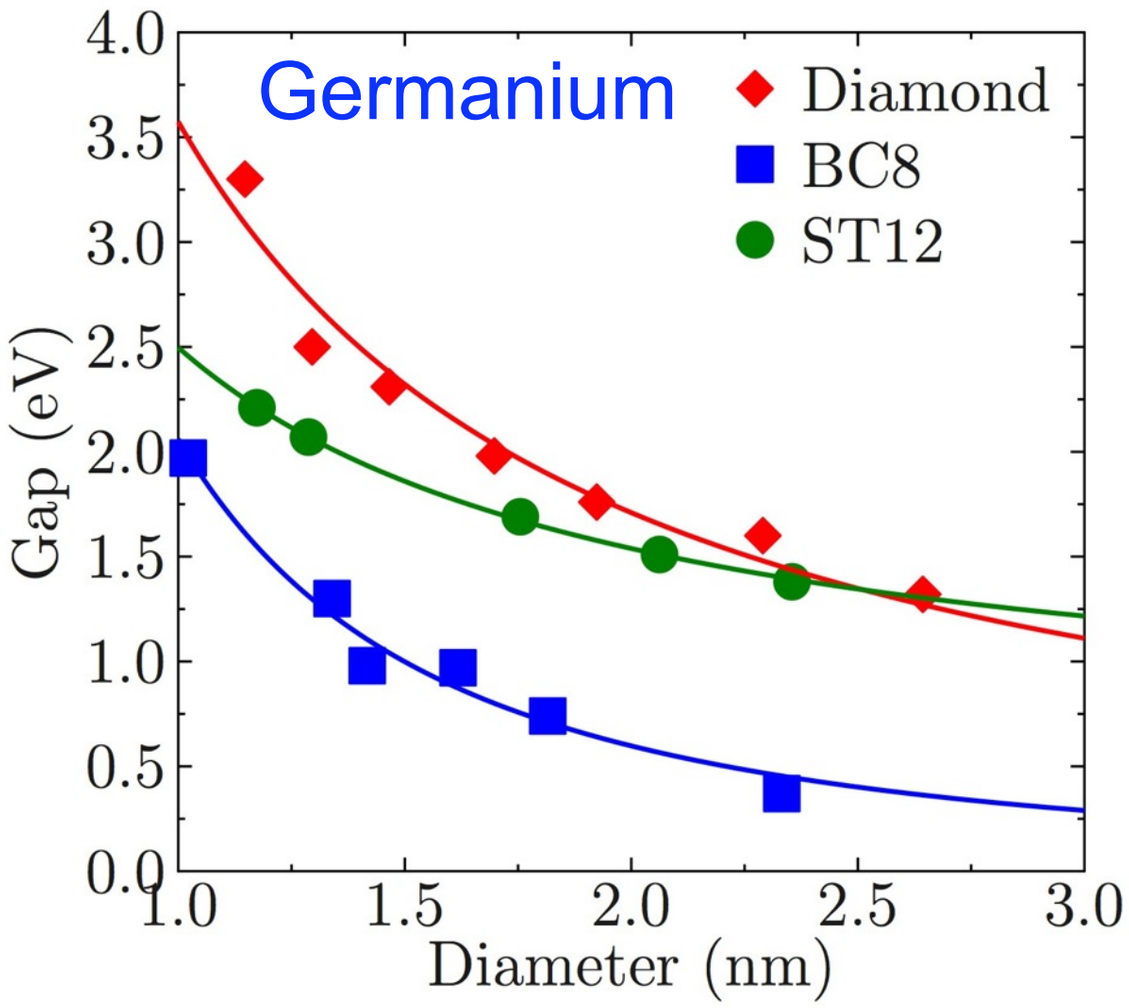

- BC8 is semimetal in the bulk, quantum confinement opens small gap in **BC8 nanocrystals => significantly reduced gaps compared to Si-I**
- Ge ST12 features reduced gaps for d < 2.5nm, significantly increased electronic density of states at band edges
- **Get realistic estimate of electronic gaps from quasiparticle calculations in GW approximation**

GW for large systems

- Calculation, storage & inversion of dielectric matrix **ε** is major computational bottleneck => spectral representation of **ε** (RPA)

$$\tilde{\epsilon} = \sum_{i=1}^{N} \tilde{\mathbf{v}}_i \lambda_i \tilde{\mathbf{v}}_i^H = \sum_{i=1}^{N} \tilde{\mathbf{v}}_i (\lambda_i - 1) \tilde{\mathbf{v}}_i^H + I$$

[4] H.-V. Nguyen, T. A. Pham, D. Rocca, G. Galli, PRB **85** 081101 (2012), PRB **87**, 155148 (2013)

GW for large systems

- Calculation, storage & inversion of dielectric matrix **ε** is major computational bottleneck => spectral representation of **ε** (RPA)

$$\tilde{\epsilon} = \sum_{i=1}^{N} \tilde{\mathbf{v}}_i \lambda_i \tilde{\mathbf{v}}_i^H = \sum_{i=1}^{N} \tilde{\mathbf{v}}_i (\lambda_i - 1) \tilde{\mathbf{v}}_i^H + I$$

- Calculating eigenvectors/-values does NOT require explicit knowledge of the matrix itself; knowing the action of **ε** on an arbitrary vector is sufficient
- In linear response: $(\epsilon - I)\Delta V_{SCF} = -v_c \Delta n$
- Charge density response Δn to perturbation of self-consistent field ΔV_{SCF} can be evaluated from density functional perturbation theory

[4] H.-V. Nguyen, T. A. Pham, D. Rocca, G. Galli, PRB **85** 081101 (2012), PRB **87**, 155148 (2013)

GW for large systems

- Calculation, storage & inversion of dielectric matrix **ε** is major computational bottleneck => spectral representation of **ε** (RPA)

$$\tilde{\epsilon} = \sum_{i=1}^{N} \tilde{\mathbf{v}}_i \lambda_i \tilde{\mathbf{v}}_i^H = \sum_{i=1}^{N} \tilde{\mathbf{v}}_i (\lambda_i - 1) \tilde{\mathbf{v}}_i^H + I$$

- Calculating eigenvectors/-values does NOT require explicit knowledge of the matrix itself; knowing the action of **ε** on an arbitrary vector is sufficient
- In linear response: $(\epsilon - I)\Delta V_{SCF} = -v_c \Delta n$
- Charge density response Δn to perturbation of self-consistent field ΔV_{SCF} can be evaluated from density functional perturbation theory
- Orthogonal iteration procedure to obtain eigen-vector/-value pairs, using ΔV_{SCF} as trial potentials
- In RPA fast monotonous decay of dielectric eigenvalue spectrum
- Single parameter N_{eig} to control numerical accuracy
- No summation over empty states, no inversion

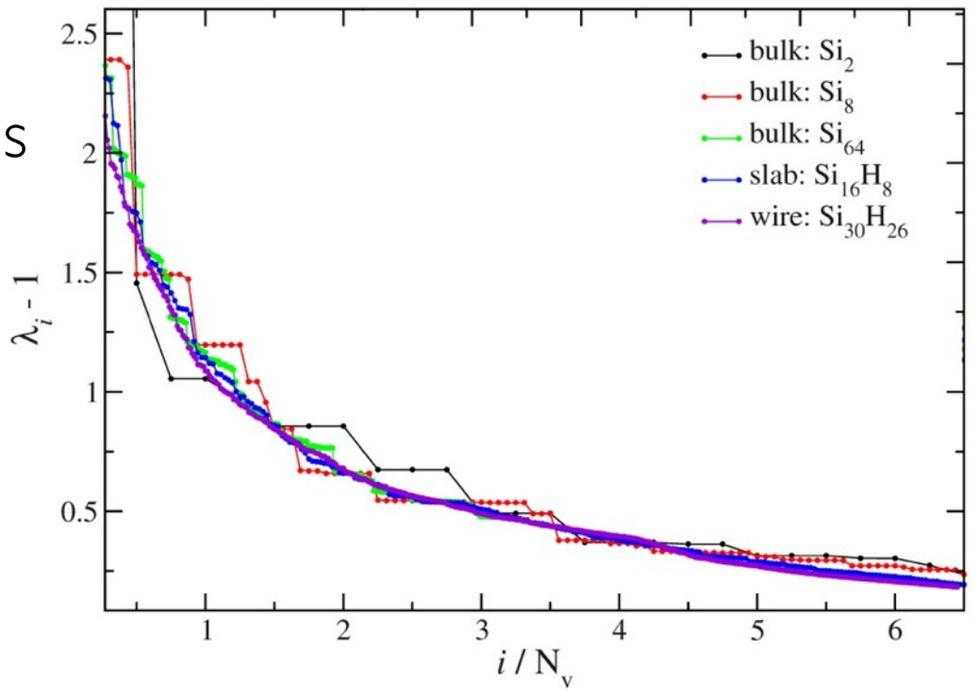

[4] H.-V. Nguyen, T. A. Pham, D. Rocca, G. Galli, PRB **85** 081101 (2012), PRB **87**, 155148 (2013)

GW for large systems

- Calculation, storage & inversion of dielectric matrix **ε** is major computational bottleneck => spectral representation of **ε** (RPA)

$$\tilde{\epsilon} = \sum_{i=1}^{N} \tilde{\mathbf{v}}_i \lambda_i \tilde{\mathbf{v}}_i^H = \sum_{i=1}^{N} \tilde{\mathbf{v}}_i (\lambda_i - 1) \tilde{\mathbf{v}}_i^H + I$$

D. Rocca, H.-V. Nguyen, T.A. Pham (UCD)

- Calculating eigenvectors/-values does NOT require explicit knowledge of the matrix itself; knowing the action of **ε** on an arbitrary vector is sufficient
- In linear response: $(\epsilon - I)\Delta V_{SCF} = -v_c \Delta n$
- Charge density response Δn to perturbation of self-consistent field ΔV_{SCF} can be evaluated from density functional perturbation theory
- Orthogonal iteration procedure to obtain eigen-vector/-value pairs, using ΔV_{SCF} as trial potentials
- In RPA fast monotonous decay of dielectric eigenvalue spectrum
- Single parameter N_{eig} to control numerical accuracy
- No summation over empty states, no inversion

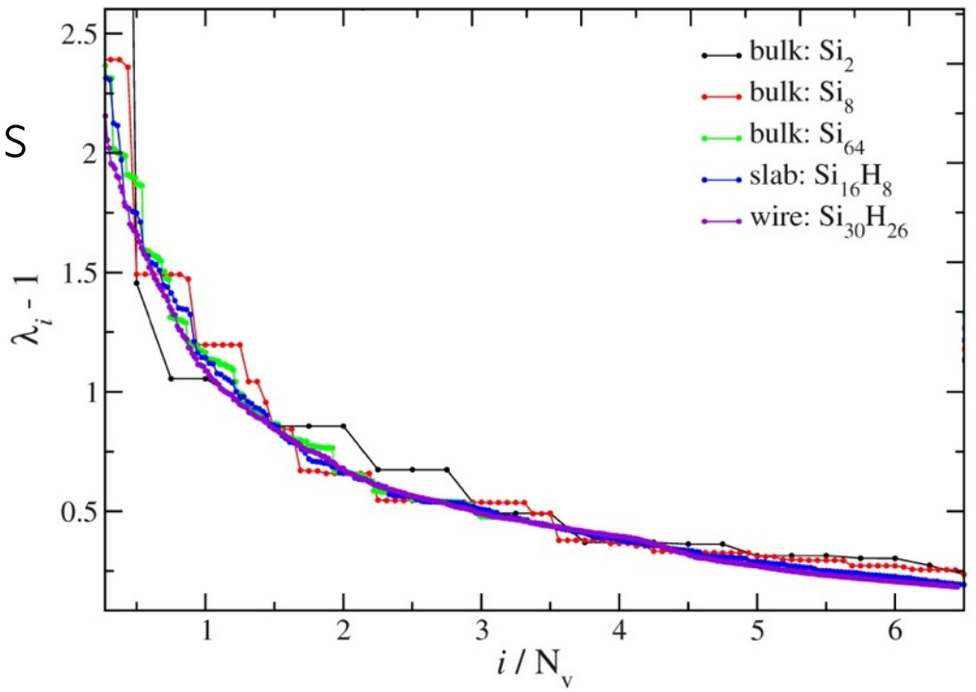

[4] H.-V. Nguyen, T.A. Pham, D. Rocca, G. Galli, PRB **85** 081101 (2012), PRB **87**, 155148 (2013)

Optimum gap for MEG in 4-8nm BC8 NPs

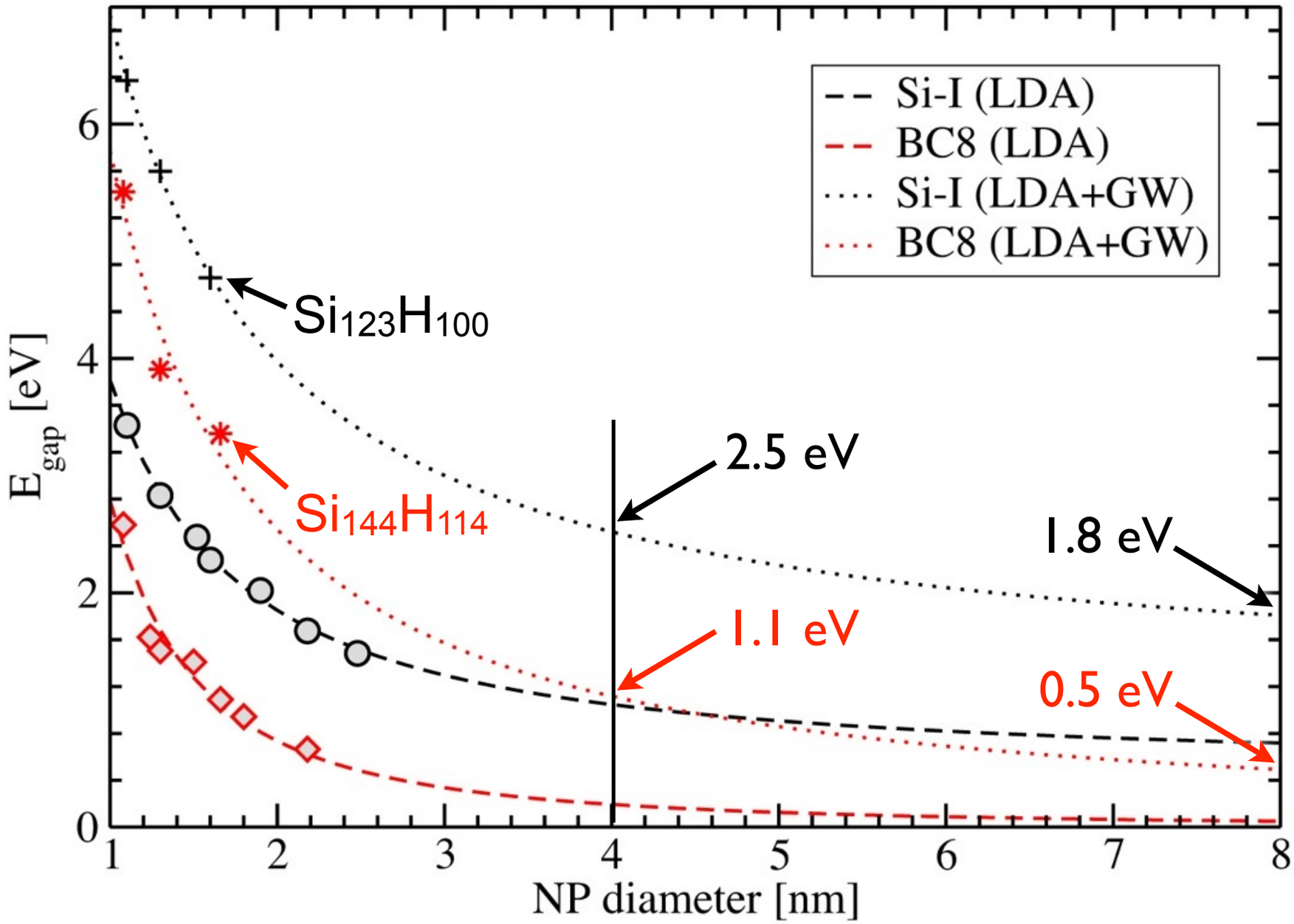

- GW calculations up to d=1.6nm ($Si_{144}H_{114}$) confirm trends observed in LDA
- **Optimum gap** for PV cells employing MEG (**E_g = 0.5-1.0 eV**) [5] found for **BC8 NPs** within typical experimental **size range of d = 4-8 nm** (extrapolation of GW gaps)

[5] M. Hanna, A. Nozik, J. Appl. Phys. **100**, 074510 (2006)

Calculating Multiple Exciton Generation (MEG) Rates

- Impact Ionization (II) is dominating contribution to MEG [6]
  => approximate MEG rates with II rates [7]
- Calculate II rates from Fermi's Golden Rule:

$$\Gamma_i^{II} = \frac{2\pi}{\hbar} \sum_f |\langle X_i | W | XX_f \rangle|^2 \, \delta(E_i - E_f)$$

- Approximate initial exciton (X_i) and final biexciton states (XX_f) as singly and doubly excited Slater determinants, built up from DFT orbitals
- Screened Coulomb interaction W calculated using same technique as during GW calculations

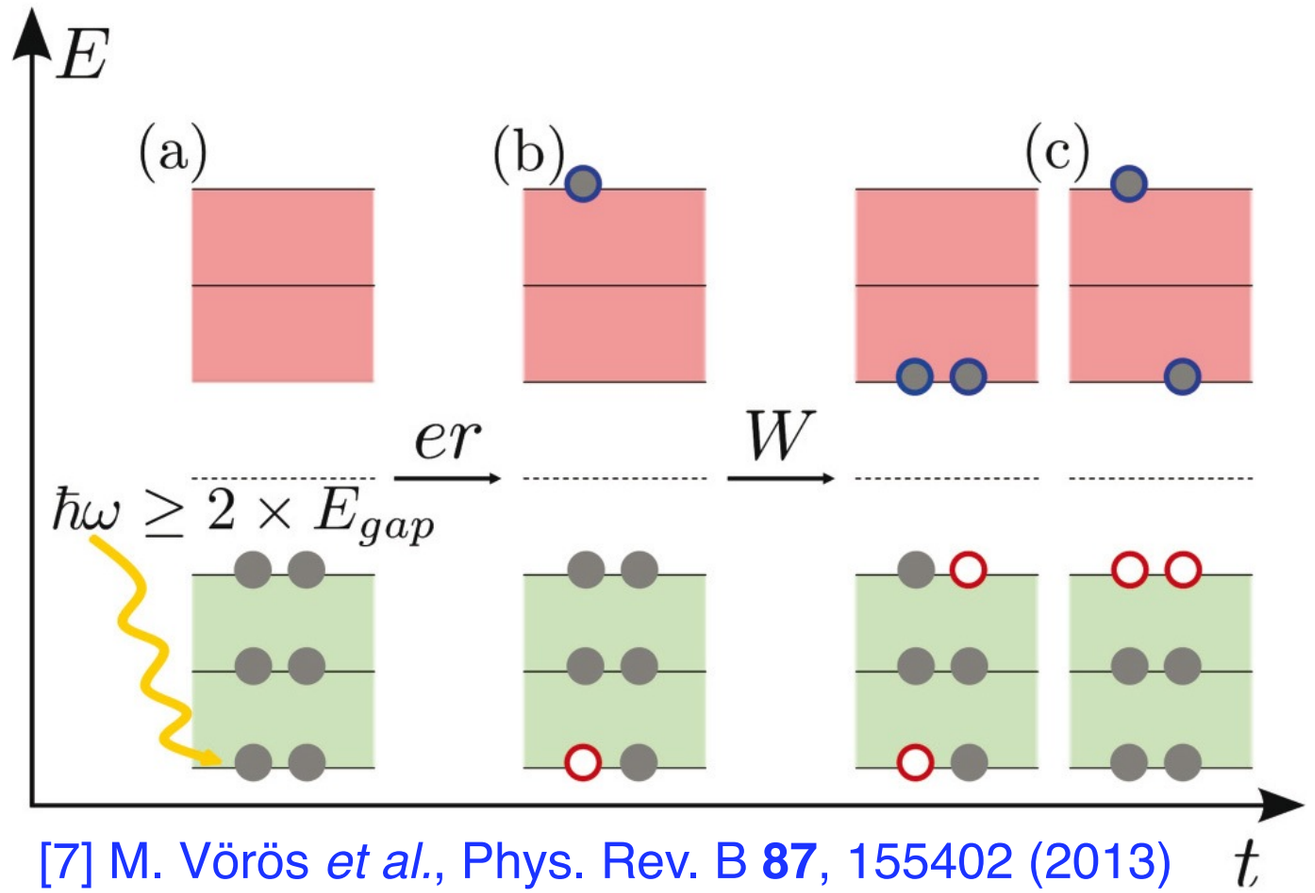

[6] A. Piryatinski *et el.*, J. Chem. Phys. **133**, 084508 (2010)
K. Velizhanin *et al.*, Phys. Rev. Lett. **106**, 207401 (2011)

[7] M. Vörös *et al.*, Phys. Rev. B **87**, 155402 (2013)

Calculating Multiple Exciton Generation (MEG) Rates

M.Vörös (UCD)

- Impact Ionization (II) is dominating contribution to MEG [6]
  => approximate MEG rates with II rates [7]
- Calculate II rates from Fermi's Golden Rule:

$$\Gamma_i^{II} = \frac{2\pi}{\hbar} \sum_f |\langle X_i | W | X X_f \rangle|^2 \, \delta(E_i - E_f)$$

- Approximate initial exciton (X_i) and final biexciton states (XX_f) as singly and doubly excited Slater determinants, built up from DFT orbitals
- Screened Coulomb interaction W calculated using same technique as during GW calculations

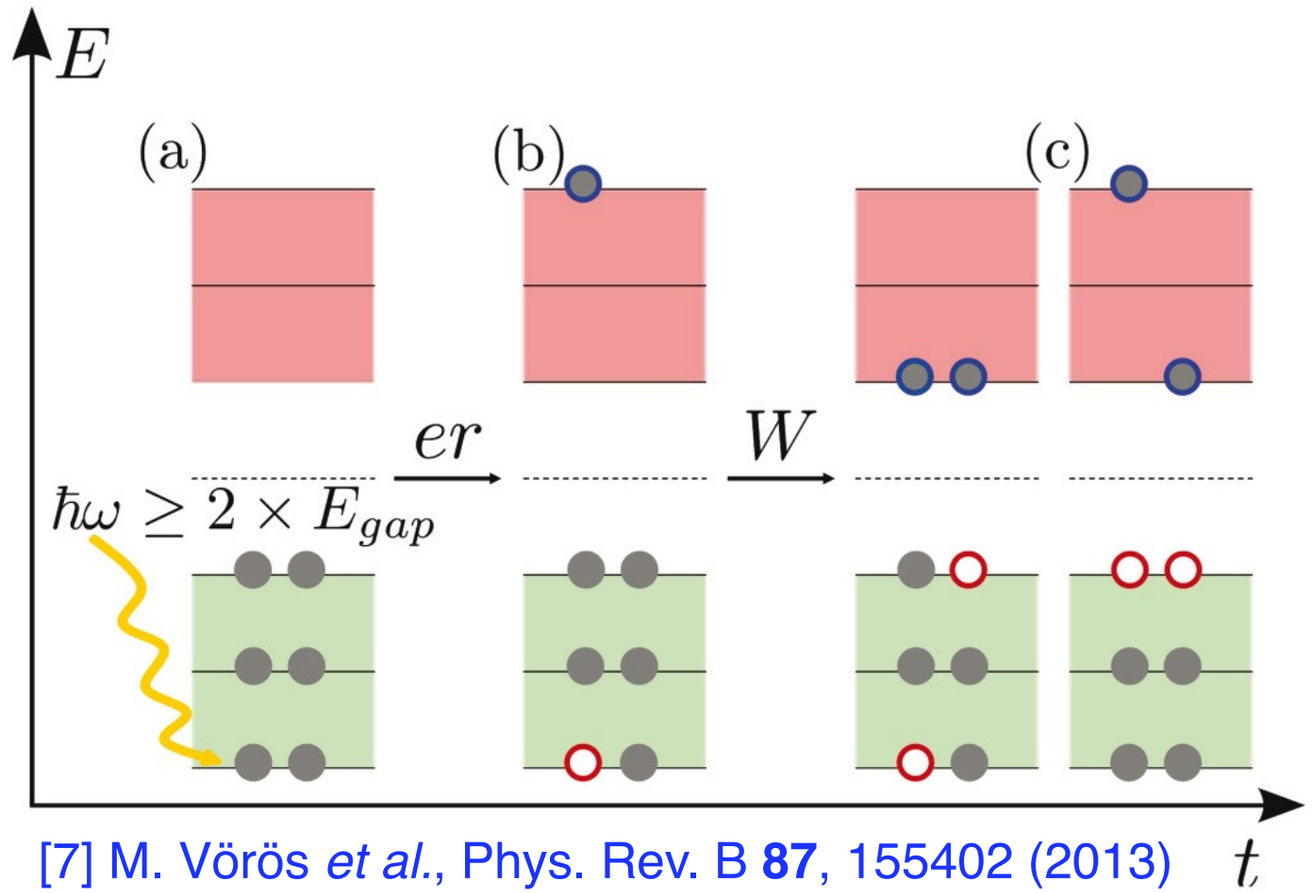

[6] A. Piryatinski *et el.*, J. Chem. Phys. **133**, 084508 (2010)
K.Velizhanin *et al.*, Phys. Rev. Lett. **106**, 207401 (2011)

[7] M. Vörös *et al.*, Phys. Rev. B **87**, 155402 (2013)

Optimum gap for MEG in 4-8nm BC8 NPs

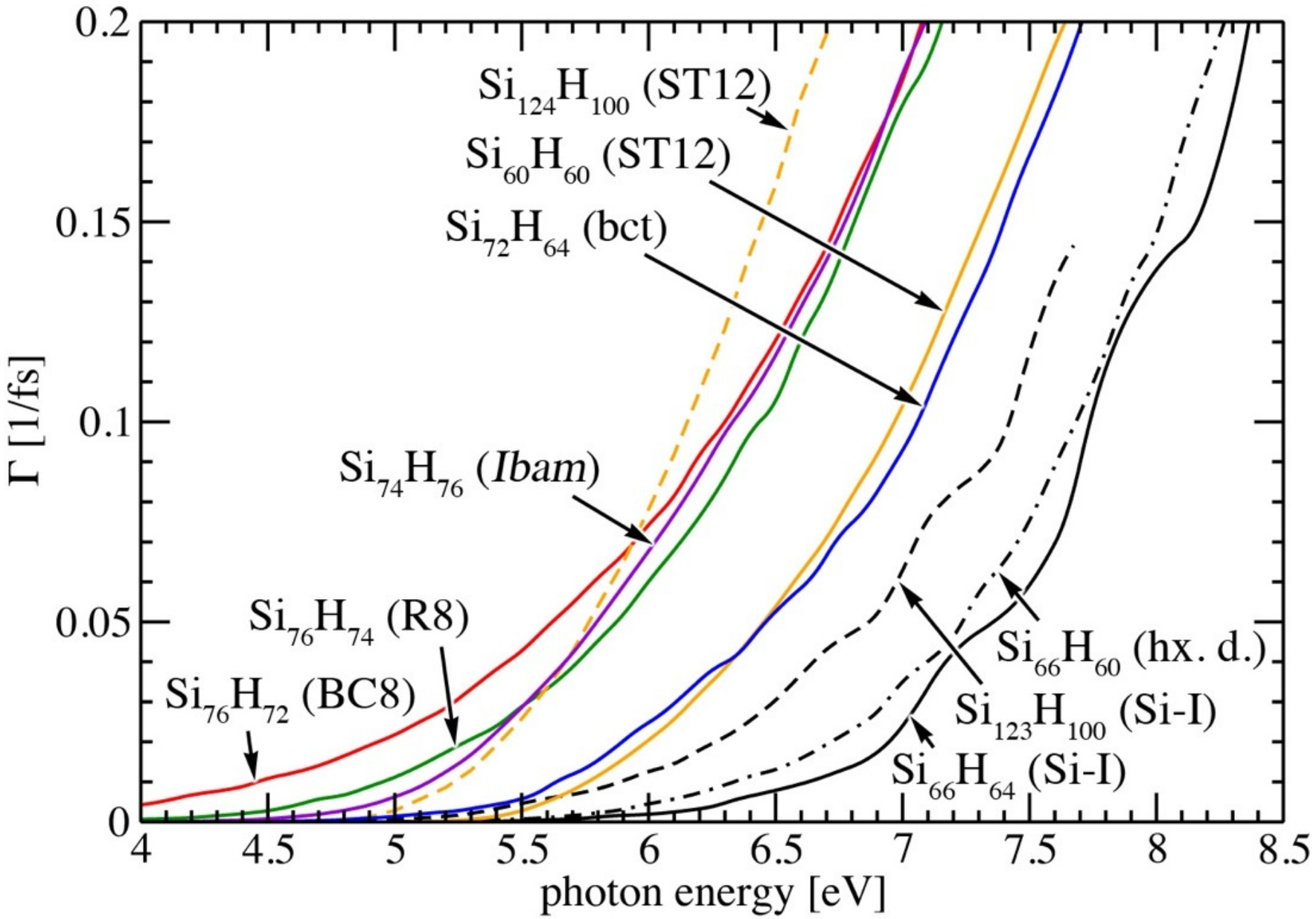

Optimum gap for MEG in 4-8nm BC8 NPs

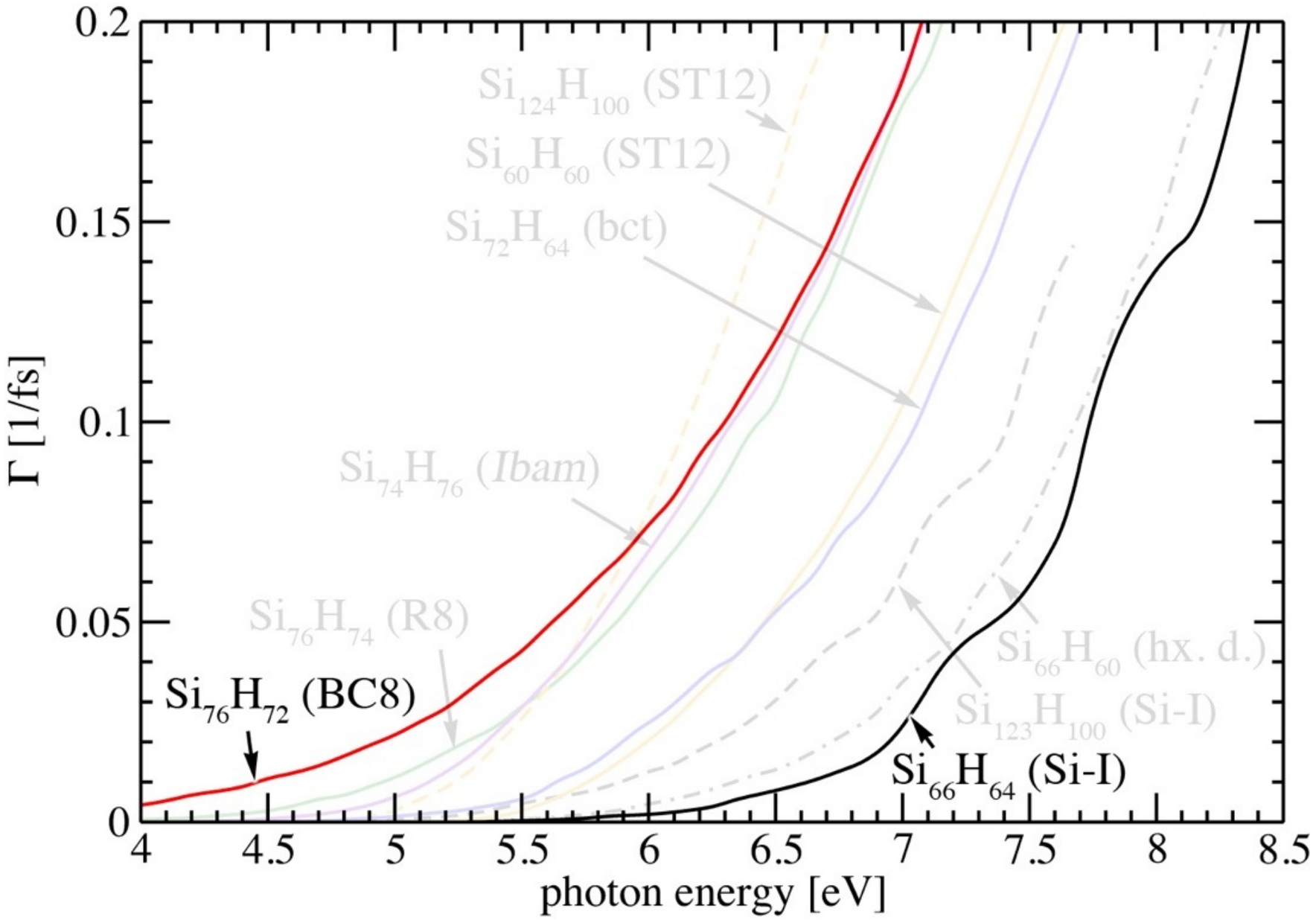

- BC8 NPs feature lower activation threshold on absolute energy scale & order of magnitude higher impact ionization rate at same energies and same NP size!

Multiple Exciton Generation in Ge allotrope nanocrystals

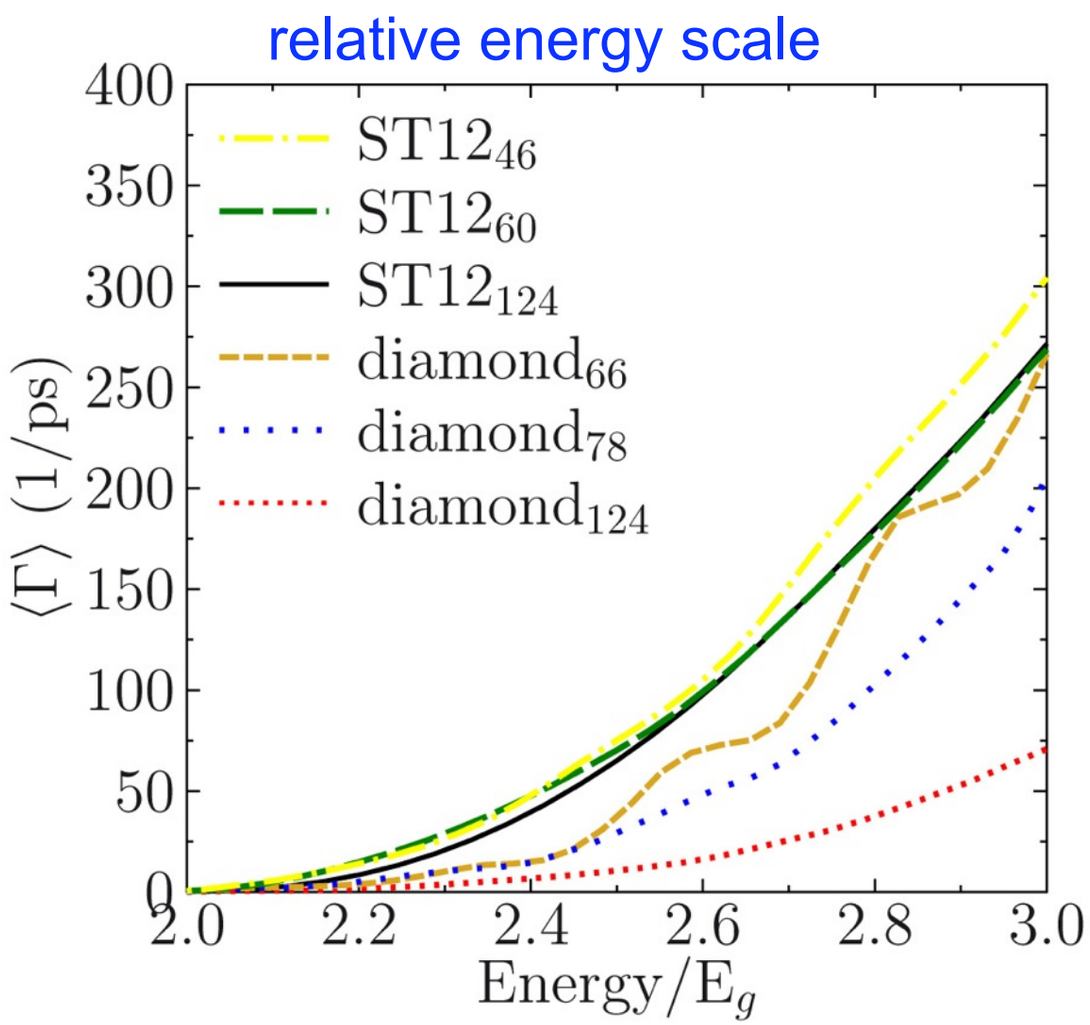

Multiple Exciton Generation in Ge allotrope nanocrystals

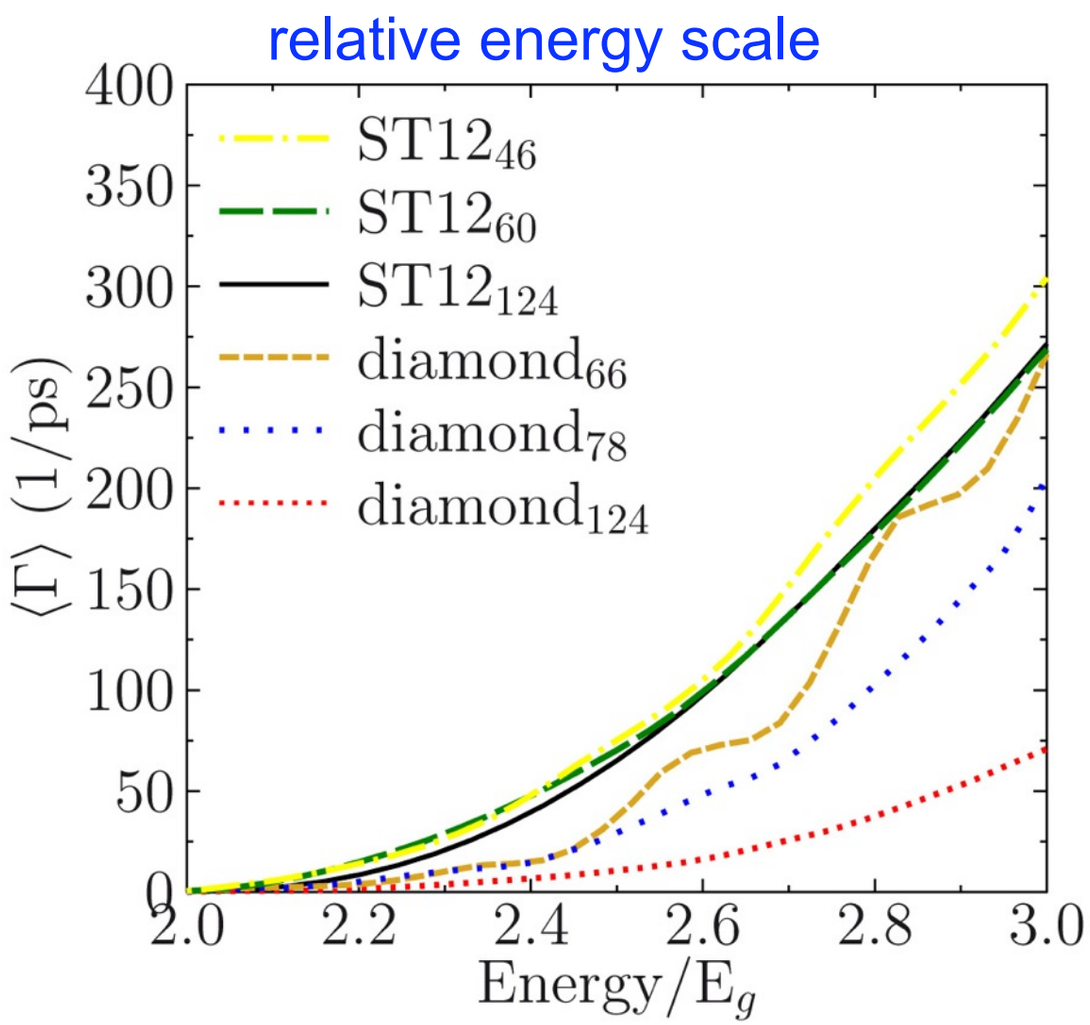

ST12 II rates size-independent

- Increasing EDOS at band edges counterbalances loss of confinement

Multiple Exciton Generation in Ge allotrope nanocrystals

relative energy scale

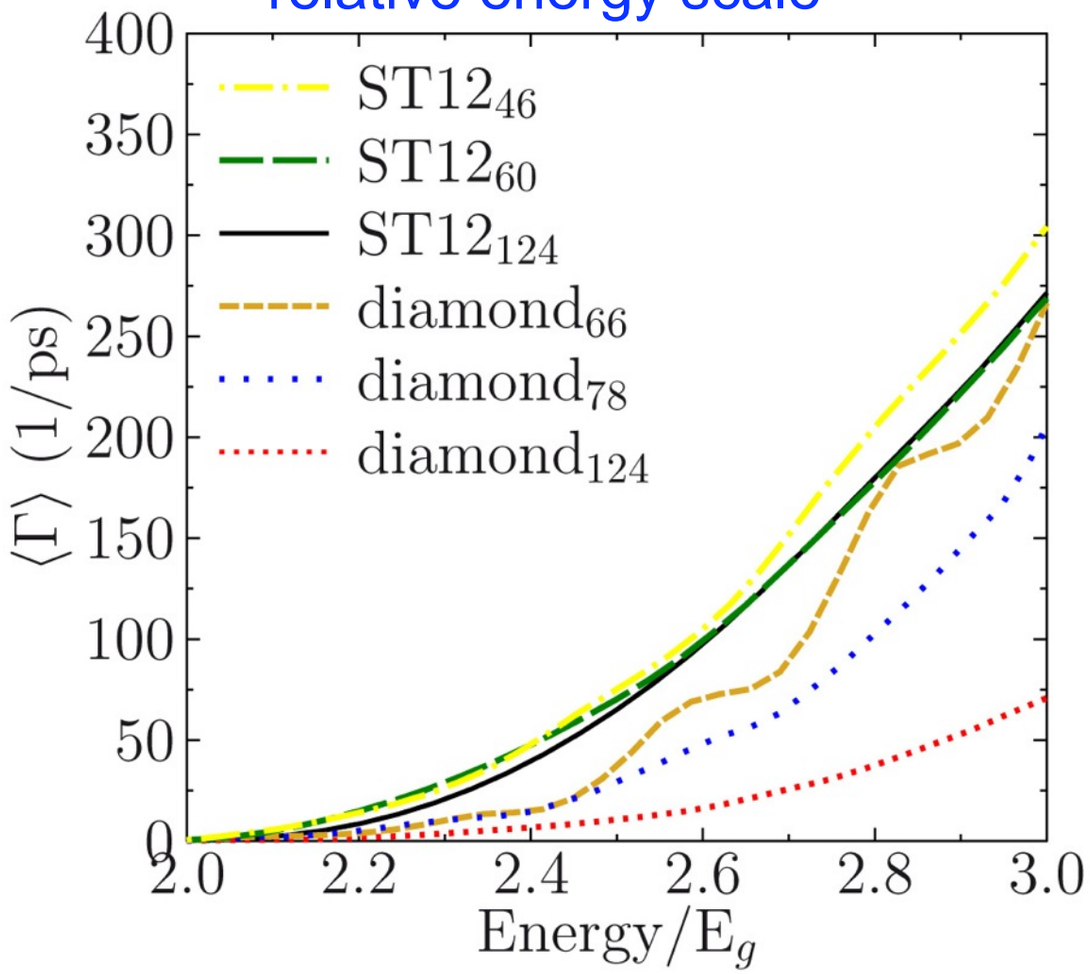

absolute energy scale

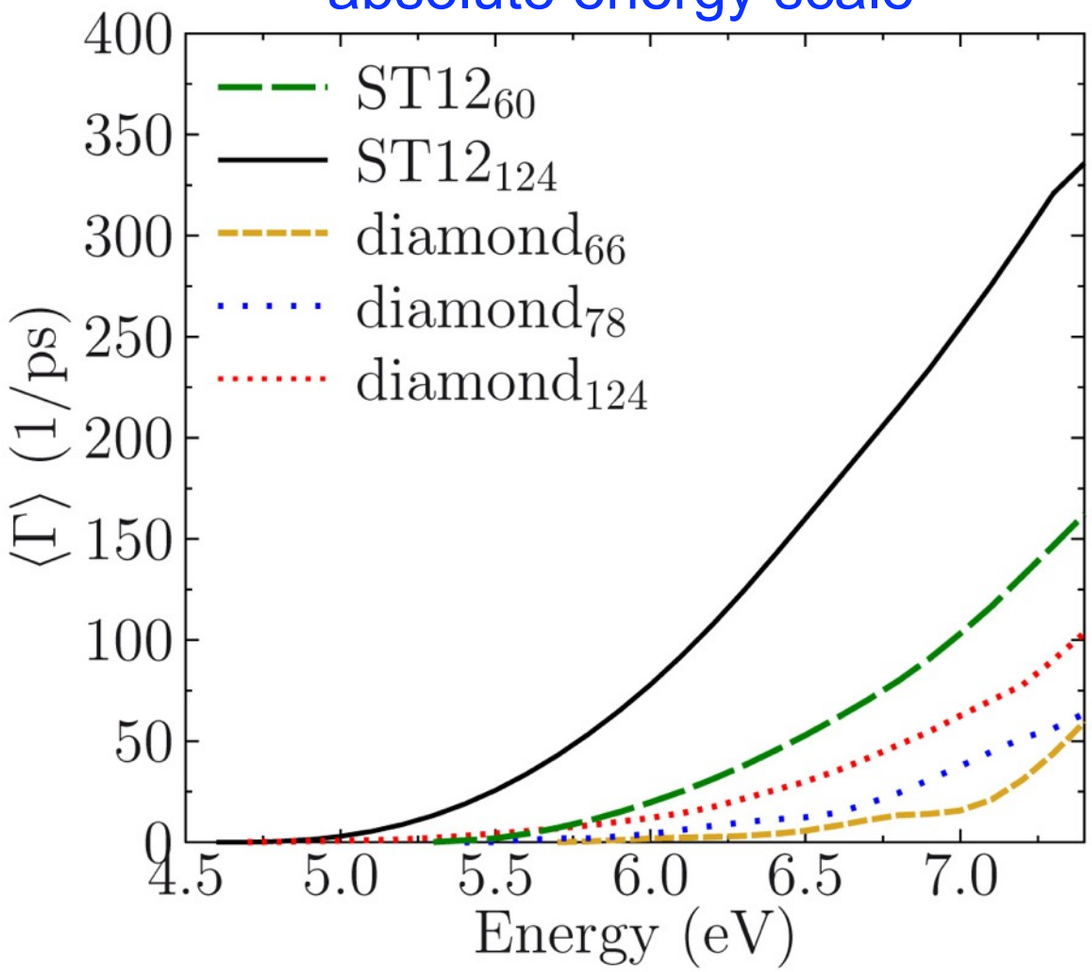

ST12 II rates size-independent

- Increasing EDOS at band edges counterbalances loss of confinement
- Simultaneously lower electronic gaps and higher relative II efficiency translate to significantly improved MEG on absolute energy scale

Summary

- **(Metastable) high pressure phases of elemental semi-conductors allow for gap engineering of nanoparticles, while retaining efficient MEG** (Si-BC8 and Ge-ST12)
- Nanoparticles with high pressure core structures can attain optimum gap range for MEG-based solar energy conversion
- High pressure nanoparticles can be formed via the high pressure route or directly at ambient pressure in solution by chemical bottom-up synthesis from a precursor

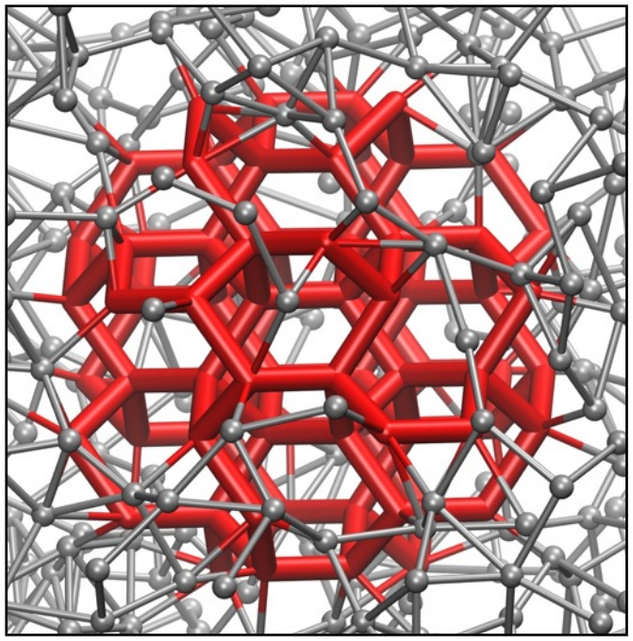

Talk on Si NPs embedded in charge transport matrix today at 12:30pm, Tre Ma

PRL **110,** 046804 (2013) PHYSICAL REVIEW LETTERS week ending 25 JANUARY 2013

High-Pressure Core Structures of Si Nanoparticles for Solar Energy Conversion

S. Wippermann,[1,2] M. Vörös,[3] D. Rocca,[1] A. Gali,[3,4] G. Zimanyi,[2] and G. Galli[1,2]
[1]*Department of Chemistry, University of California, Davis, California 95616, USA*
[2]*Department of Physics, University of California, Davis, California 95616, USA*
[3]*Department of Atomic Physics, Budapest University of Technology and Economics, Budafoki út 8, H-1111 Budapest, Hungary*
[4]*Institute for Solid State Physics and Optics, Wigner Research Center for Physics, Hungarian Academy of Sciences, P.O. Box 49, H-1525 Budapest, Hungary*
(Received 1 August 2012; published 24 January 2013)

Acknowledgements

Giulia Galli and her group at UChicago, especially Marton Vörös and Tuan Anh Pham

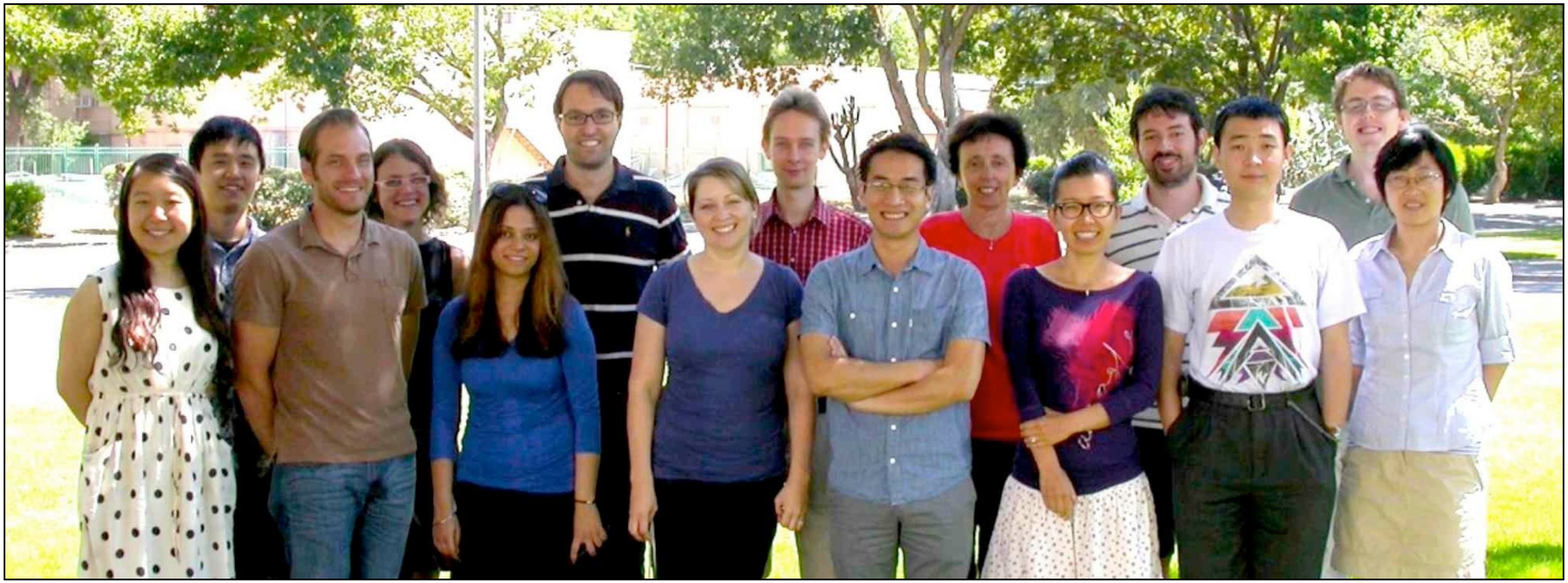

Francois Gygi (UC Davis), Gergely Zimanyi (UC Davis),
Adam Gali (Budapest Univ.), Dario Rocca (Univ. Lorraine)

Bundesministerium für Bildung und Forschung — NanoMatFutur 13N12972

Deutsche Forschungsgemeinschaft DFG — Wi3879/1-1

NERSC — NISE-project 35687

NSF — NSF/Solar DMR-1035468

Max-Planck-Institute for Iron Research, Düsseldorf

Additional Slides

Optical properties (TD-DFT RPA)

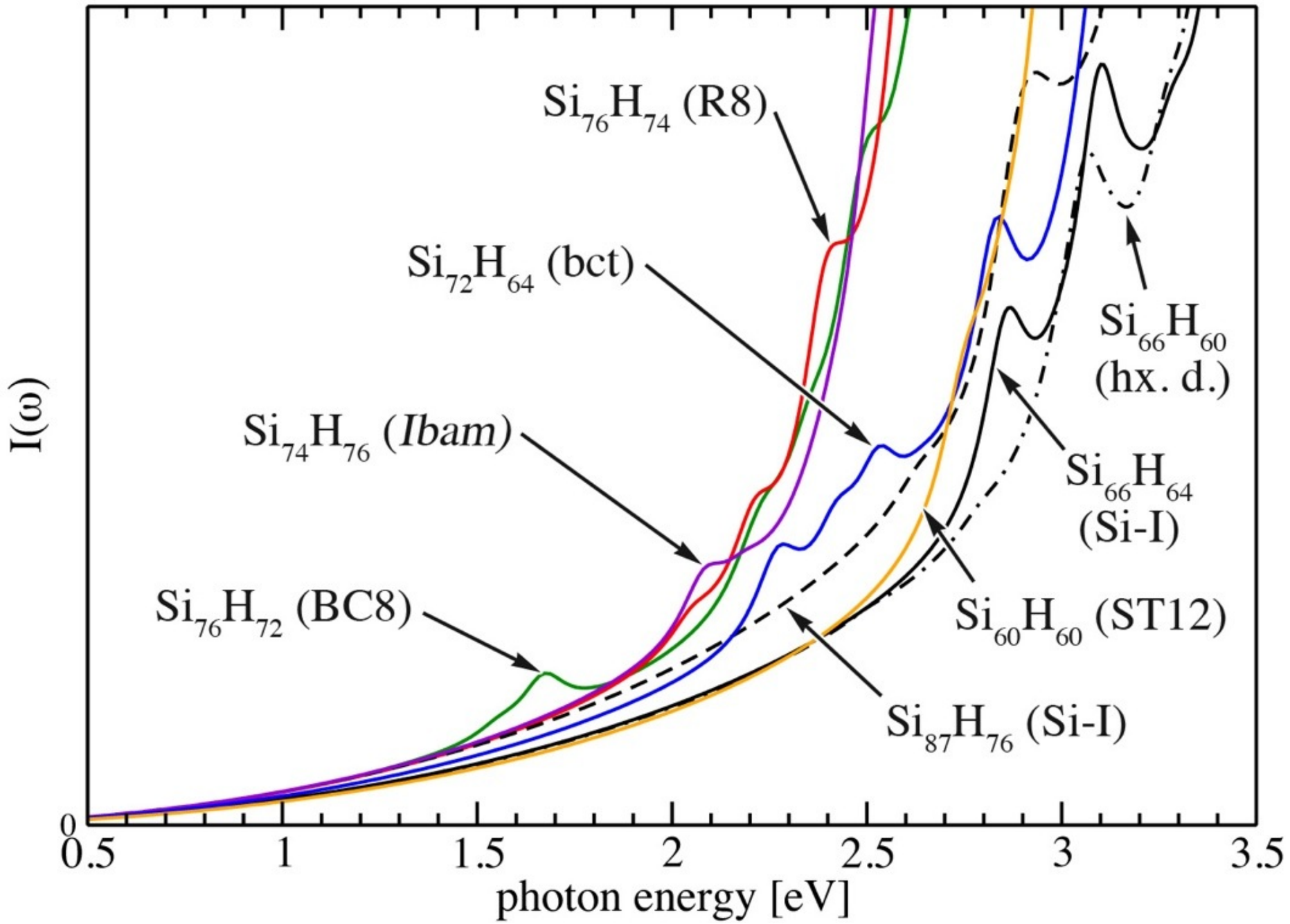

- **red-shifted optical absorption** onset for high density phases (BC8, R8, *Ibam*)
- less pronounced for ST12 and low density phases (bct, hd)

cubic diamond vs. ST12

$$\Gamma_i^{II} = \frac{2\pi}{\hbar} \sum_f |\langle X_i | W | XX_f \rangle|^2 \, \delta(E_i - E_f)$$
$$= \frac{2\pi}{\hbar} \left| W_{eff}^i \right|^2 \cdot TDOS_i$$

- **cubic diamond:** NP size increase reduces Coulomb interaction W_{eff}, trion DOS almost constant

  => impact ionization rate drops

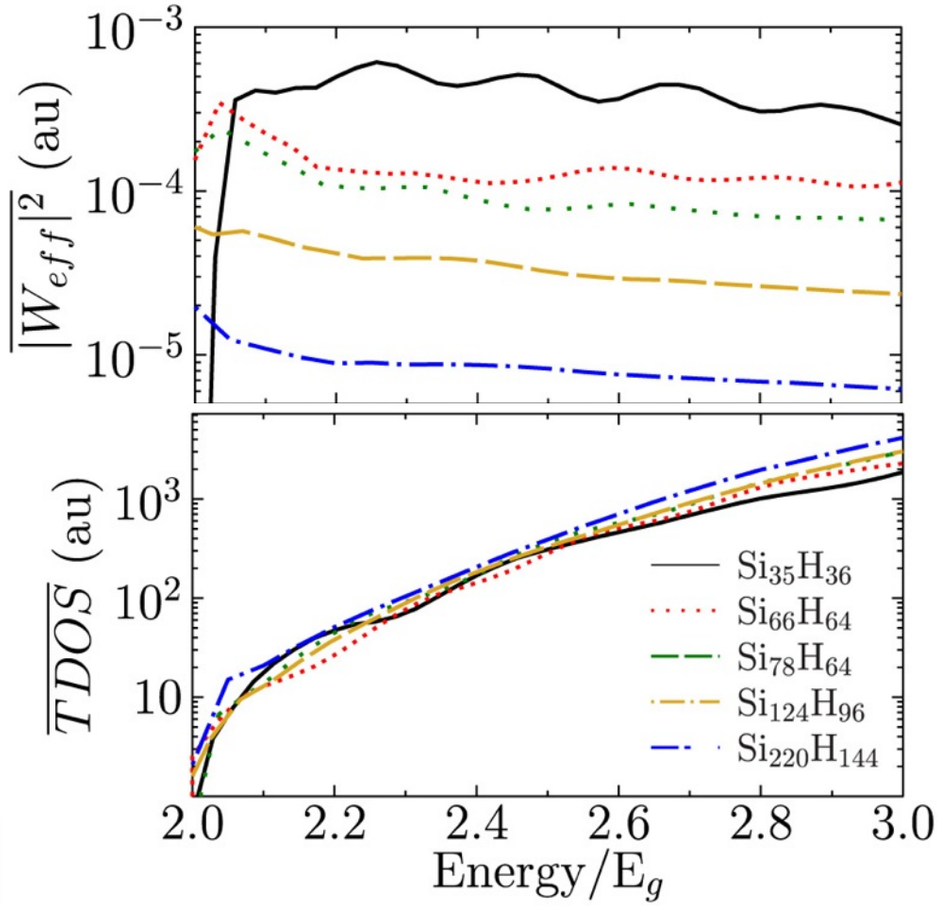

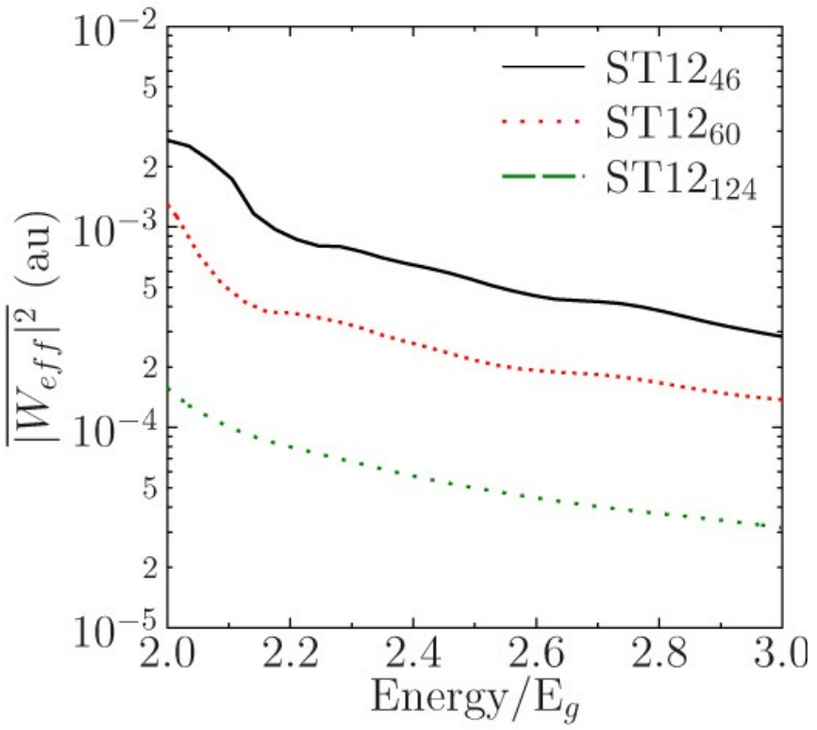

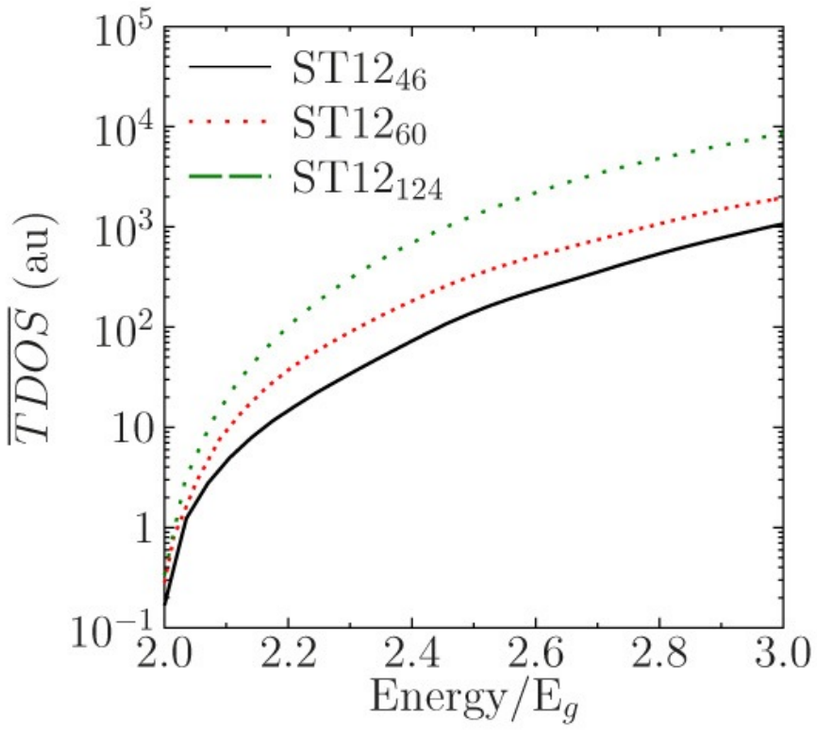

- **ST12:** W_{eff} reduced as for cubic diamond, ***but TDOS increases***

  => impact ionization rate remains almost constant with increasing size

Density functional theory (DFT):

- Hohenberg-Kohn theorem:

$$E_{XC}[n] \approx E_{XC}^{LDA}[n] = \int n(\boldsymbol{r}) \epsilon_{XC}^{hom}(n(\boldsymbol{r})) d\boldsymbol{r}$$

$$E_e[n] = T_0[n] + \frac{1}{2} \int \frac{n(\boldsymbol{r}) n(\boldsymbol{r}')}{|\boldsymbol{r} - \boldsymbol{r}'|} d\boldsymbol{r} d\boldsymbol{r}' + \int n(\boldsymbol{r}) V(\boldsymbol{r}) d\boldsymbol{r} + E_{XC}[n]$$

atomic positions

[Walter Kohn, Nobel Prize for chemistry in 1998]

Density functional theory (DFT):

Hohenberg-Kohn theorem:

$$E_{XC}[n] \approx E_{XC}^{LDA}[n] = \int n(\boldsymbol{r}) \epsilon_{XC}^{hom}(n(\boldsymbol{r})) d\boldsymbol{r}$$

$$E_e[n] = T_0[n] + \frac{1}{2} \int \frac{n(\boldsymbol{r}) n(\boldsymbol{r}')}{|\boldsymbol{r} - \boldsymbol{r}'|} d\boldsymbol{r} d\boldsymbol{r}' + \int n(\boldsymbol{r}) V(\boldsymbol{r}) d\boldsymbol{r} + E_{XC}[n]$$

atomic positions

[Walter Kohn, Nobel Prize for chemistry in 1998]

Kohn-Sham self-consistent electron structure

$$\left\{ -\frac{\nabla^2}{2} + \int \frac{n(\boldsymbol{r}')}{|\boldsymbol{r} - \boldsymbol{r}'|} d\boldsymbol{r}' + V(\boldsymbol{r}) + \frac{\delta E_{XC}^{LDA}}{\delta n(\boldsymbol{r})} \right\} \psi_j(\boldsymbol{r}) = \epsilon_j \psi_j(\boldsymbol{r})$$

$$n(\boldsymbol{r}) = \sum_j^{occ.} |\psi_j(\boldsymbol{r})|^2$$

Density functional theory (DFT):

Hohenberg-Kohn theorem:

$$E_{XC}[n] \approx E_{XC}^{LDA}[n] = \int n(\boldsymbol{r}) \epsilon_{XC}^{hom}(n(\boldsymbol{r})) d\boldsymbol{r}$$

$$E_e[n] = T_0[n] + \frac{1}{2} \int \frac{n(\boldsymbol{r}) n(\boldsymbol{r}')}{|\boldsymbol{r} - \boldsymbol{r}'|} d\boldsymbol{r} d\boldsymbol{r}' + \int n(\boldsymbol{r}) V(\boldsymbol{r}) d\boldsymbol{r} + E_{XC}[n]$$

[Walter Kohn, Nobel Prize for chemistry in 1998]

atomic positions

Starting point: initial geometry

⬇

external potential

interatomic forces

Kohn-Sham self-consistent electron structure

$$\left\{ -\frac{\nabla^2}{2} + \int \frac{n(\boldsymbol{r}')}{|\boldsymbol{r} - \boldsymbol{r}'|} d\boldsymbol{r}' + V(\boldsymbol{r}) + \frac{\delta E_{XC}^{LDA}}{\delta n(\boldsymbol{r})} \right\} \psi_j(\boldsymbol{r}) = \epsilon_j \psi_j(\boldsymbol{r})$$

$$n(\boldsymbol{r}) = \sum_j^{occ.} |\psi_j(\boldsymbol{r})|^2$$

⬇

structurally relaxed ground-state

Density functional theory (DFT):

Hohenberg-Kohn theorem:

$$E_{XC}[n] \approx E_{XC}^{LDA}[n] = \int n(\boldsymbol{r}) \epsilon_{XC}^{hom}(n(\boldsymbol{r})) d\boldsymbol{r}$$

$$E_e[n] = T_0[n] + \frac{1}{2} \int \frac{n(\boldsymbol{r}) n(\boldsymbol{r}')}{|\boldsymbol{r} - \boldsymbol{r}'|} d\boldsymbol{r} d\boldsymbol{r}' + \int n(\boldsymbol{r}) V(\boldsymbol{r}) d\boldsymbol{r} + E_{XC}[n]$$

[Walter Kohn, Nobel Prize for chemistry in 1998]

atomic positions

Starting point: initial geometry

external potential

interatomic forces

Kohn-Sham self-consistent electron structure

$$\left\{ -\frac{\nabla^2}{2} + \int \frac{n(\boldsymbol{r}')}{|\boldsymbol{r} - \boldsymbol{r}'|} d\boldsymbol{r}' + V(\boldsymbol{r}) + \frac{\delta E_{XC}^{LDA}}{\delta n(\boldsymbol{r})} \right\} \psi_j(\boldsymbol{r}) = \epsilon_j \psi_j(\boldsymbol{r})$$

$$n(\boldsymbol{r}) = \sum_j^{occ.} |\psi_j(\boldsymbol{r})|^2$$

structurally relaxed ground-state

- vibrational and thermal properties
- electronic properties
- spectroscopic and transport properties

Excited states (GW/BSE)

- DFT disregards screened e^-–e^- interaction and e^-–h interaction for excited states => band gap underestimation, wrong distribution of spectral weights

Excited states (GW/BSE)

- DFT disregards screened e^-–e^- interaction and e^-–h interaction for excited states => band gap underestimation, wrong distribution of spectral weights
- Perturbative approaches for including screening (GW) and e^-–h interaction (Bethe-Salpeter), starting from Quantum Liouville equation

$$i\frac{d\hat{\rho}(t)}{dt} = \left[\hat{\mathcal{H}}(t), \hat{\rho}(t)\right] \qquad \rho(\mathbf{r},\mathbf{r}',t) = \sum_v \phi_v^*(\mathbf{r},t)\phi_v(\mathbf{r}',t)$$

single particle occ. orbitals

$$\int \hat{\mathcal{H}}(\mathbf{r},\mathbf{r}',t)\phi(\mathbf{r}',t)d\mathbf{r}' = \left(-\frac{1}{2}\nabla^2 + v_H(\mathbf{r},t) + v_{ext}(\mathbf{r},t)\right)\phi(\mathbf{r},t) + \int \Sigma(\mathbf{r},\mathbf{r}',t)\phi(\mathbf{r}',t)d\mathbf{r}'$$

time-dep. perturbation, i. e. electromagn. field

Excited states (GW/BSE)

- DFT disregards screened e^-–e^- interaction and e^-–h interaction for excited states => band gap underestimation, wrong distribution of spectral weights
- Perturbative approaches for including screening (GW) and e^-–h interaction (Bethe-Salpeter), starting from Quantum Liouville equation

$$i\frac{d\hat{\rho}(t)}{dt} = \left[\hat{\mathcal{H}}(t), \hat{\rho}(t)\right] \qquad \rho(\mathbf{r},\mathbf{r}',t) = \sum_v \phi_v^*(\mathbf{r},t)\phi_v(\mathbf{r}',t)$$

single particle occ. orbitals

$$\int \hat{\mathcal{H}}(\mathbf{r},\mathbf{r}',t)\phi(\mathbf{r}',t)d\mathbf{r}' = \left(-\frac{1}{2}\nabla^2 + v_H(\mathbf{r},t) + v_{ext}(\mathbf{r},t)\right)\phi(\mathbf{r},t) + \int \Sigma(\mathbf{r},\mathbf{r}',t)\phi(\mathbf{r}',t)d\mathbf{r}'$$

time-dep. perturbation, i. e. electromagn. field

self-energy

$$\Sigma_{COH}(\mathbf{r},\mathbf{r}') = \frac{1}{2}\delta(\mathbf{r}-\mathbf{r}')W_p(\mathbf{r},\mathbf{r}')$$
$$\Sigma_{SEX}(\mathbf{r},\mathbf{r}',t) = -\sum_v \phi_v(\mathbf{r},t)\phi_v^*(\mathbf{r}',t)W(\mathbf{r},\mathbf{r}')$$

statically screened Bethe-Salpeter equation (BSE)

Excited states (GW/BSE)

- DFT disregards screened e^-–e^- interaction and e^-–h interaction for excited states => band gap underestimation, wrong distribution of spectral weights
- Perturbative approaches for including screening (GW) and e^-–h interaction (Bethe-Salpeter), starting from Quantum Liouville equation

$$i\frac{d\hat{\rho}(t)}{dt} = \left[\hat{\mathcal{H}}(t), \hat{\rho}(t)\right] \qquad \rho(\mathbf{r},\mathbf{r}',t) = \sum_v \phi_v^*(\mathbf{r},t)\phi_v(\mathbf{r}',t)$$

single particle occ. orbitals

$$\int \hat{\mathcal{H}}(\mathbf{r},\mathbf{r}',t)\phi(\mathbf{r}',t)d\mathbf{r}' = \left(-\frac{1}{2}\nabla^2 + v_H(\mathbf{r},t) + v_{ext}(\mathbf{r},t)\right)\phi(\mathbf{r},t) + \int \Sigma(\mathbf{r},\mathbf{r}',t)\phi(\mathbf{r}',t)d\mathbf{r}'$$

time-dep. perturbation, i. e. electromagn. field

self-energy

$$\Sigma_{COH}(\mathbf{r},\mathbf{r}') = \frac{1}{2}\delta(\mathbf{r}-\mathbf{r}')W_p(\mathbf{r},\mathbf{r}')$$

$$\Sigma_{SEX}(\mathbf{r},\mathbf{r}',t) = -\sum_v \phi_v(\mathbf{r},t)\phi_v^*(\mathbf{r}',t)W(\mathbf{r},\mathbf{r}')$$

statically screened Bethe-Salpeter equation (BSE)

screened Coulomb interaction

Excited states (GW/BSE)

- To correct for DFT's band gap underestimation, quasiparticle energies can be obtained in GW approximation from

$$\Sigma_{GW}(\mathbf{r},\mathbf{r}';i\omega) = \frac{1}{2\pi}\int G(\mathbf{r},\mathbf{r}';i(\omega-\omega'))W(\mathbf{r},\mathbf{r}';i\omega')d\omega'$$

Excited states (GW/BSE)

- To correct for DFT's band gap underestimation, quasiparticle energies can be obtained in GW approximation from

$$\Sigma_{GW}(\mathbf{r},\mathbf{r}';i\omega) = \frac{1}{2\pi}\int G(\mathbf{r},\mathbf{r}';i(\omega-\omega'))W(\mathbf{r},\mathbf{r}';i\omega')d\omega'$$

- Screened Coulomb interaction required (in random phase (RPA) approx.)

$$W(\mathbf{r},\mathbf{r}') = \int \epsilon^{-1}(\mathbf{r},\mathbf{r}'')v_c(\mathbf{r}'',\mathbf{r}')d\mathbf{r}''$$

Excited states (GW/BSE)

- To correct for DFT's band gap underestimation, quasiparticle energies can be obtained in GW approximation from

$$\Sigma_{GW}(\mathbf{r},\mathbf{r}';i\omega) = \frac{1}{2\pi}\int G(\mathbf{r},\mathbf{r}';i(\omega-\omega'))W(\mathbf{r},\mathbf{r}';i\omega')d\omega'$$

- Screened Coulomb interaction required (in random phase (RPA) approx.)

$$W(\mathbf{r},\mathbf{r}') = \int \epsilon^{-1}(\mathbf{r},\mathbf{r}'')v_c(\mathbf{r}'',\mathbf{r}')d\mathbf{r}''$$

- Bottleneck: calculation, storage & inversion of dielectric matrix is very computationally demanding, involves large sums over empty states and is hard to converge

Excited states (GW/BSE)

- To correct for DFT's band gap underestimation, quasiparticle energies can be obtained in GW approximation from

$$\Sigma_{GW}(\mathbf{r},\mathbf{r}';i\omega) = \frac{1}{2\pi}\int G(\mathbf{r},\mathbf{r}';i(\omega-\omega'))W(\mathbf{r},\mathbf{r}';i\omega')d\omega'$$

- Screened Coulomb interaction required (in random phase (RPA) approx.)

$$W(\mathbf{r},\mathbf{r}') = \int \epsilon^{-1}(\mathbf{r},\mathbf{r}'')v_c(\mathbf{r}'',\mathbf{r}')d\mathbf{r}''$$

- Bottleneck: calculation, storage & inversion of dielectric matrix is very computationally demanding, involves large sums over empty states and is hard to converge
- Solution: spectral representation of RPA dielectric matrix; obtain matrix from directly calculating eigenvectors and eigenvalues

$$\tilde{\epsilon} = \sum_{i=1}^{N} \tilde{\mathbf{v}}_i \lambda_i \tilde{\mathbf{v}}_i^H = \sum_{i=1}^{N} \tilde{\mathbf{v}}_i (\lambda_i - 1)\tilde{\mathbf{v}}_i^H + I$$

=> no summation over empty states, no inversion, storage of eigenvector/-value pairs only!

How to calculate the screening

- Obtaining the eigenvectors/-values does NOT require explicit knowledge of the matrix; knowledge of the action of the matrix on an arbitrary vector is sufficient!
- in linear response: $(\epsilon - I)\Delta V_{SCF} = -v_c \Delta n$
- charge density response Δn to perturbation of self-consist. field ΔV_{SCF} can be evaluated from density functional perturbation theory

$$\tilde{\epsilon} = \sum_{i=1}^{N} \tilde{\mathbf{v}}_i \lambda_i \tilde{\mathbf{v}}_i^H = \sum_{i=1}^{N} \tilde{\mathbf{v}}_i (\lambda_i - 1) \tilde{\mathbf{v}}_i^H + I$$

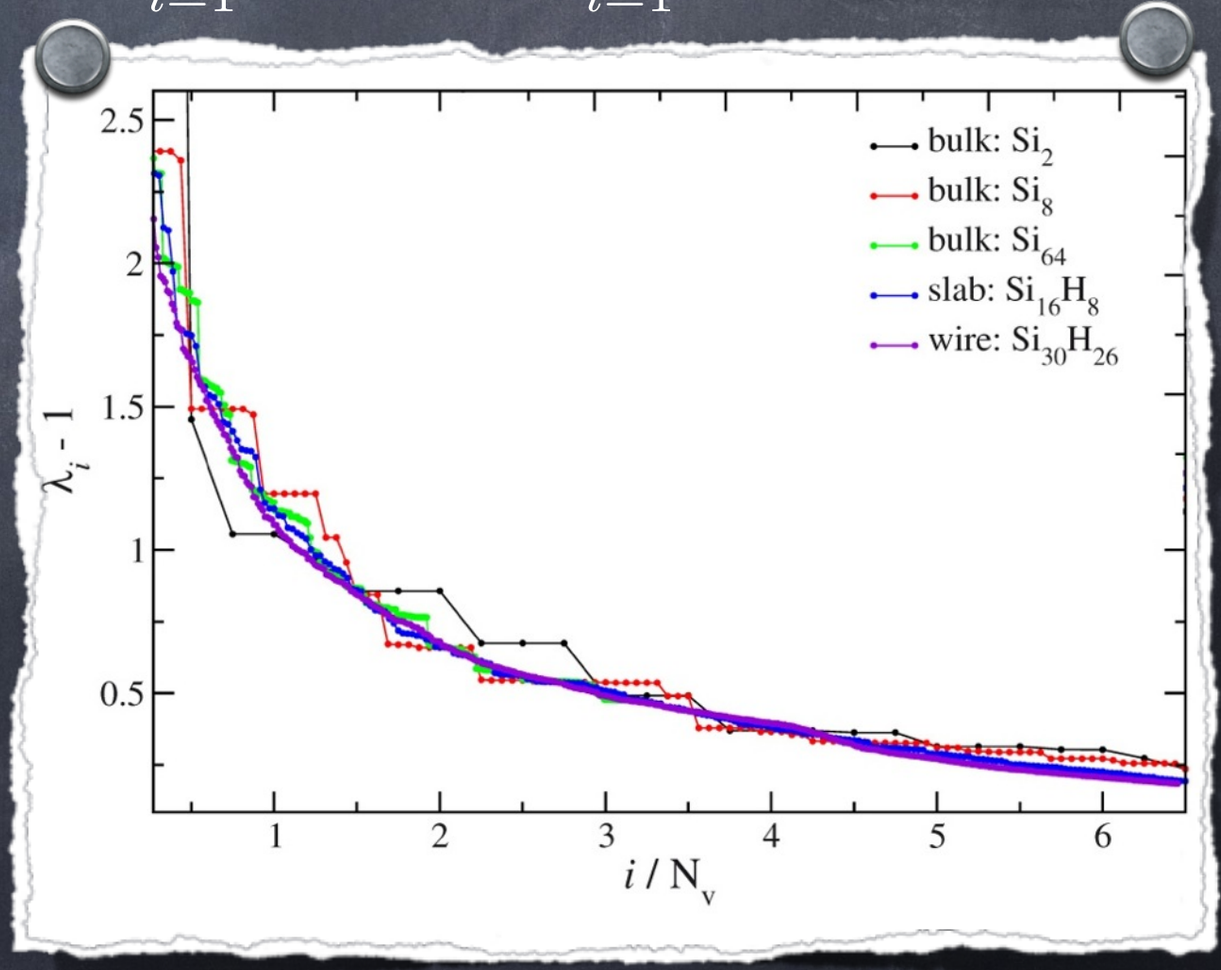

- orthogonal iteration procedure to obtain eigenvectors/-values, using ΔV_{SCF} as trial potentials
- in RPA fast monotonous decay of dielectric eigenvalue spectrum
- single parameter N_{eig} to control numerical accuracy

[H. Wilson *et al.*, PRB **79**, 245106 (2009); D. Rocca *et al.*, J. Chem. Phys. **133**, 164109 (2010); H.-V. Nguyen *et al.*, PRB **85**, 081101 (2012)]